The Continuing Utility and Potential of Nb-based Superconducting composite wires

Subtitle: What have Nb-based SC done for you lately?

Mike Sumption,
(The Ohio State University)

..And Slides from (and thanks to!):
A Kikuchi
I Kresgin
C Senatore
C. Tarantini/M.Mandal

And some additional borrowings from "the literature"..
K. Schlenga
B Seeber

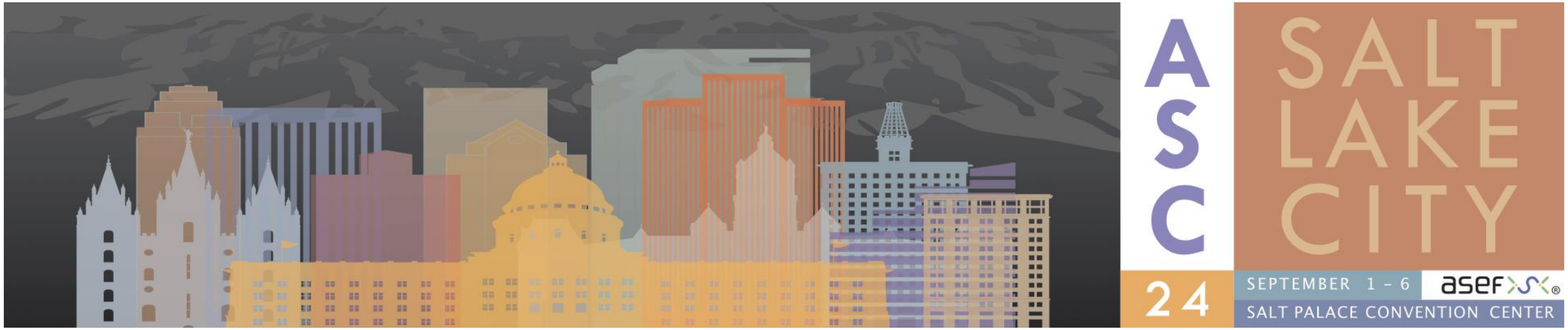

Sept 1-6, 2024, Salt Lake City

IEEE-CSC, ESAS and CSSJ SUPERCONDUCTIVITY NEWS FORUM (global edition), Issue No. 57, Oct 2024. Presentation given at ASC 2024, Sept 2024, Salt Lake City, Utah, USA.

Are LTSC (Especially Nb-based) still relevant?

- Exciting developments continue for HTS conductors, including ReBCO, Bi:2212, MgB_2, and the pnictides
- However, Nb-based superconductors, including NbTi, Nb_3Sn, Nb_3Al, continue in their utility and potential
- NbTi conductors are important commercially (MRI and NMR), and various particle accelerators rely on them
- LTSCs will continue to be used wherever and whenever they can be, because they are cost effective, mature, and convenient (except for the cooling!)
- Nb_3Sn conductors continue to have potential for the next generation of accelerator magnets as the most cost effective and practical solution for achieving the needed performance
- End if solely LTSC accelerator magnets are supplemented by HTS inserts, LTSC will be crucial aspects of the machine, keeping them viable both technically and cost-wise
- Recent advances in Nb_3Sn are quite exciting and performance continues to increase for this well known conductor
- New versions of Nb_3Sn as well as Nb_3Al may interesting applications in specialty magnets, insertion devices, and other roles
- LTSC conductor, especially those based on Nb, will continue to be of interest for machine and application development for some time to come.

IEEE-CSC, ESAS and CSSJ SUPERCONDUCTIVITY NEWS FORUM (global edition), Issue No. 57, Oct 2024. Presentation given at ASC 2024, Sept 2024, Salt Lake City, Utah, USA.

NbTi

Where do we find it at this conference? In the *Magnet Sessions*

- MRI, sure, to be dominated by NbTi for the forseeable future
- Electron Ion Collider
- Role in Muon collider?
- Proton therapy gantries
- Maglev (transportation transformation)
- Wind energy
- Quantum computing

IEEE-CSC, ESAS and CSSJ SUPERCONDUCTIVITY NEWS FORUM (global edition), Issue No. 57, Oct 2024. Presentation given at ASC 2024, Sept 2024, Salt Lake City, Utah, USA.

Electron Ion Collider

Sure, existing accelerators with SC magnets are NbTi based, but even new ones (EIC) and some magnets of projected ones (Muon collider) rely on NbTi

NbTi based superconducting Magnets

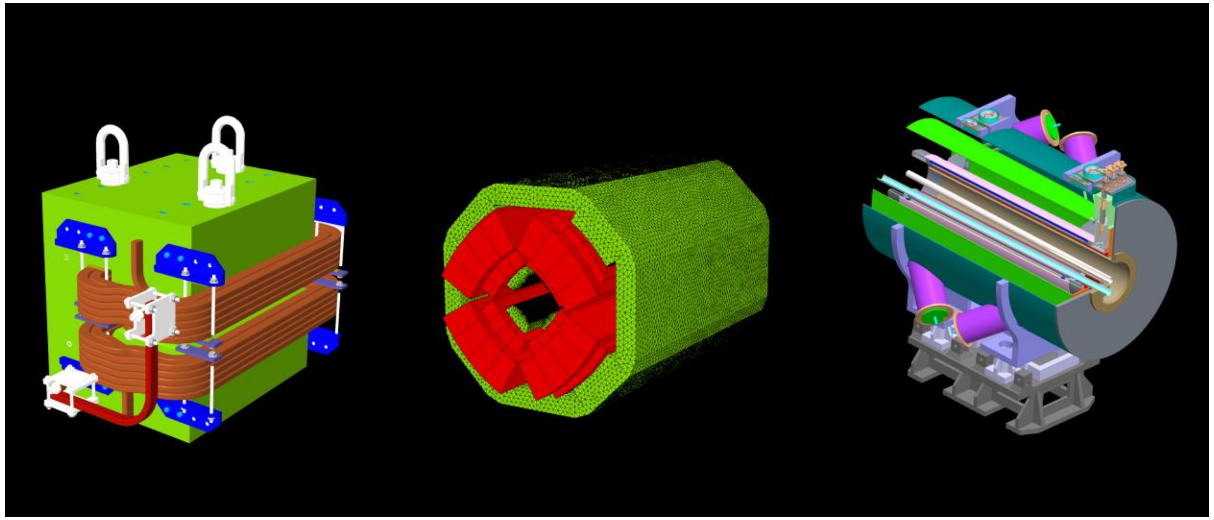

IEEE-CSC, ESAS and CSSJ SUPERCONDUCTIVITY NEWS FORUM (global edition), Issue No. 57, Oct 2024. Presentation given at ASC 2024, Sept 2024, Salt Lake City, Utah, USA.

Wind energy

LTSC appears to be commercially competitive from this (and other) analyses

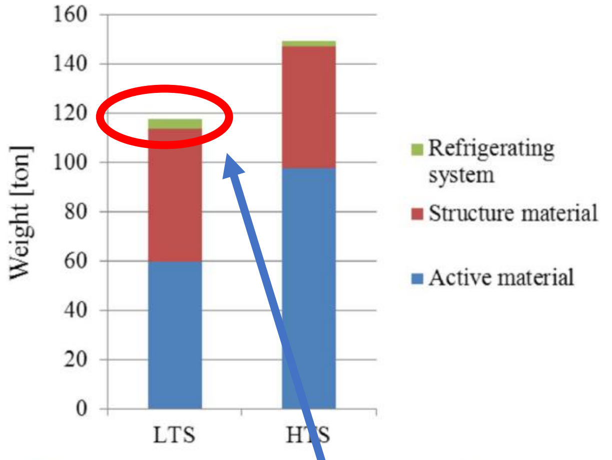

Fig. 9. Weight comparison of the designed LTS and HTS wind generators.

TABLE III
COMPARISON OF THREE KINDS OF HTS TAPES

Items	Bi2223	Bi2212	YBCO
Critical Temp.	110 K	80 K	92 K
Practical working temp.	< 30 K	< 30 K	< 30 K
Cooling medium	Cold He gas, LNe or LH	Cold He gas, LNe or LH	Cold He gas, LNe or LH
Bc2 (4.2 K)	>100 T	>100 T	>100 T
Applied magnetic field	< 2 T @77 K < 20 T @4.2 K	20-50 T @4.2K	< 3 T @77 K > 25T@4.2K
Anisotropic	Strong	No	Strong
Max rated tensile stress	~ 270 MPa	> 250 MPa	> 550 MPa
Jc (A/mm^2)	~ 500 @(77 K, self field)	> 7000 @(4.2 K, self field)	3x10^5@(77 K, self field)
Je (A/mm^2)	~ 150 @(77 K, self field) ~ 180 @(20 K,5 T⊥) > 300 @(20 K,10 T//)	>1000 @(4.2 K, 0 T) 266 @(4.2 K, 45 T)	> 200 @(77 K, self field) > 400 @(20 K, 5 T⊥) > 1000 @(20 K, 10 T//)
Price (2012)	40-50 $/kAm @20 K, 120-150 $/kAm@77 K	40-50 $/kAm @20 K, 120-150 $/kAm@77K	80-150$/kAm @20 K, 300-500 $/kAm@77 K
Dimensions	4.5mm*0.3mm	Custom	3-12mm *0.05-0.2mm
Technology maturity	High	High	High
Commercialization	Mass production	Minor production	Initial production

TABLE IV
COMPARISON OF THREE KINDS OF LTS WIRES

Items	NbTi	Nb_3Sn	MgB_2
Critical Temp.	9.6 K	18 K	39 K
Practical working temperature	< 6 K	< 6 K	20-25 K
Cooling medium	LHe	LHe	LH or Condiction
Bc2 (4.2 K)	~13 T	~25 T	18 T
Applied magnetic field	< 10 T	< 23.5 T	< 18 T
Anisotropic	No	No	No
Max rated tensile stress	> 800 MPa	> 360 MPa	> 100 MPa
Jc (A/mm^2)	~ 3000 @(4.2K,5T)	~ 6000 @(4.2K,10T)	~ 1000 @(4.2K,10T)
Je (A/mm^2)	< 1000 @(4.2K,5T)	< 1000 @(4.2K,10T)	~ 167 @(4.2K,10T)
Price (2012)	1-2 $/kAm @4.2 K	~15 $/kAm @4.2 K	~ 5 $/kAm @20 K
Dimensions	Custom	Custom	Custom
Technology maturity	High	High	low
Commercialization	Mass production	Mass production	Initial production

LTSC in this analysis, outperforms HTS

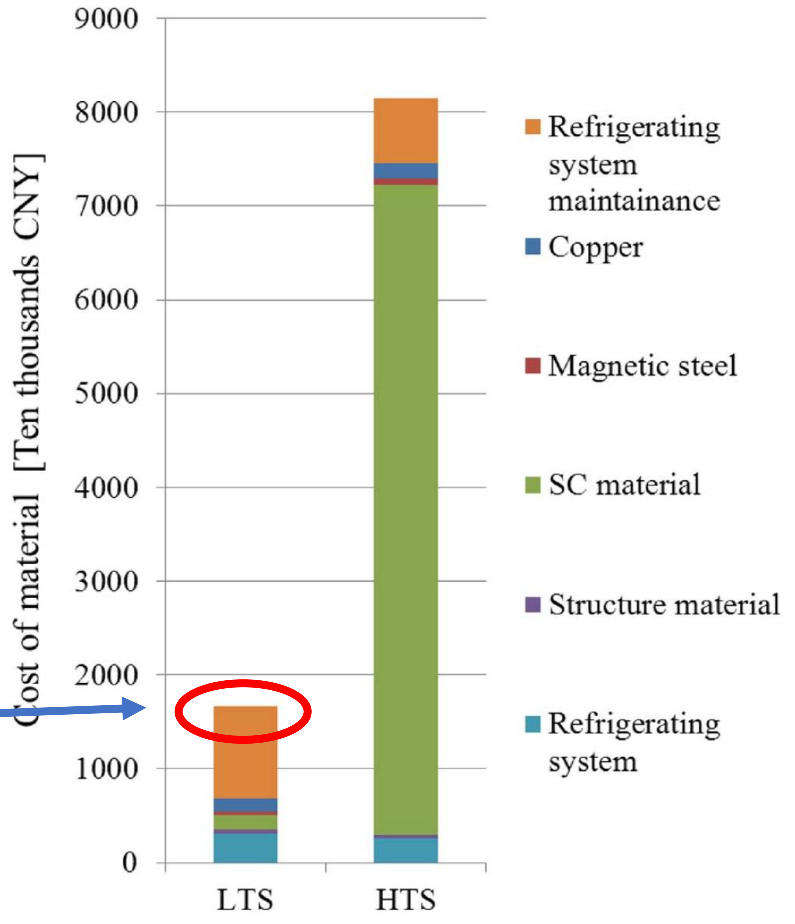

Fig. 11. Cost comparison of the designed LTS and HTS wind generators. (In a sequence from top to bottom, the six items of the legend indicate the subsections of the column diagrams successively.).

EEE TRANSACTIONS ON APPLIED SUPERCONDUCTIVITY, VOL. 25, NO. 3, JUNE 2015 5201806

Comparison Study of Superconducting Wind Generators With HTS and LTS Field Windings

Jin Wang, *Member, IEEE*, Ronghai Qu, *Senior Member, IEEE*, Yingzhen Liu, Jie He, Zhe Zhu, and Haiyang Fang

Quantum computing interconnects

Fig. 1. Eight-trace Maybell cable prototype manufactured using linearly actuated mechanical stage with laser welding. Two sheets of 1 mil thick NbTi foil are welded around PFA-coated NbTi wires with a continuous laser weld.

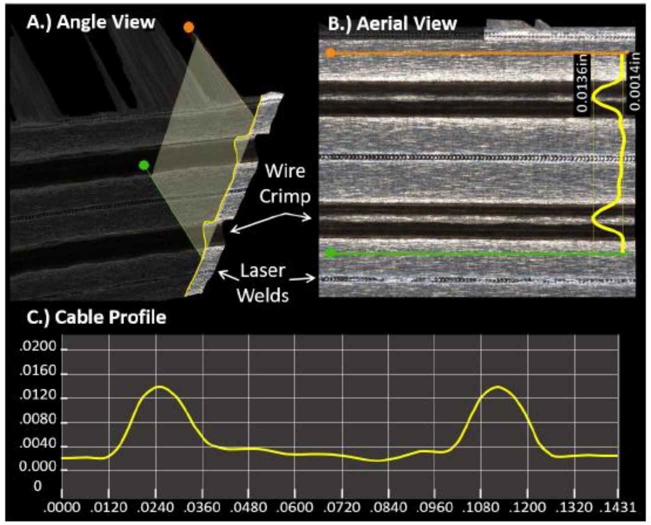

Fig. 2. Manufacturing data obtained from JT Automation during a prototype cable manufacturing run. A.) Angle view showing a single sheet of NbTi foil with two crimps made to house wires with continuous laser welds in-between. B.) Aerial view of the NbTi foil showing the same welds and crimps pictured to the left. C.) Cable profile measured in inches. In all views the cable profile is highlighted in yellow.

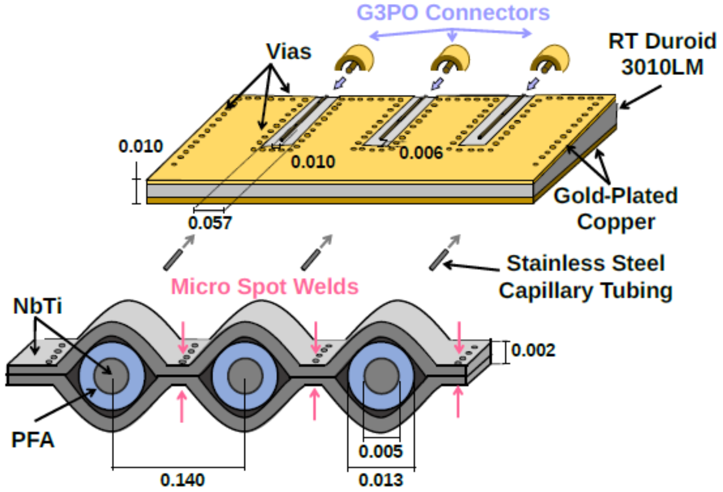

Improved Flexible Coaxial Ribbon Cable for High-Density Superconducting Arrays

Jennifer Pearl Smith *, Benjamin A. Mazin *, Alirio Boaventura†, Kyle J. Thompson†, Miguel Daal *
*University of California Santa Barbara, Department of Physics and Astronomy, Santa Barbara, CA 93106 USA
(email: jennifer_smith@ucsb.edu) †Maybell Quantum Industries, Denver, CO 80221 USA

Nb_3Sn

- Either sole magnets or background for HTS magnets for FCC
- Possible Role in Muon Collider magnets
- Proton therapy accelerator magnets (Mevion)
- Fusion ITER, DEMO, (now competing with ReBCO!)
- Undulators
- Energy Storage?

IEEE-CSC, ESAS and CSSJ SUPERCONDUCTIVITY NEWS FORUM (global edition), Issue No. 57, Oct 2024. Presentation given at ASC 2024, Sept 2024, Salt Lake City, Utah, USA.

Nb_3Sn and NbTi potential for some muon collider magnets

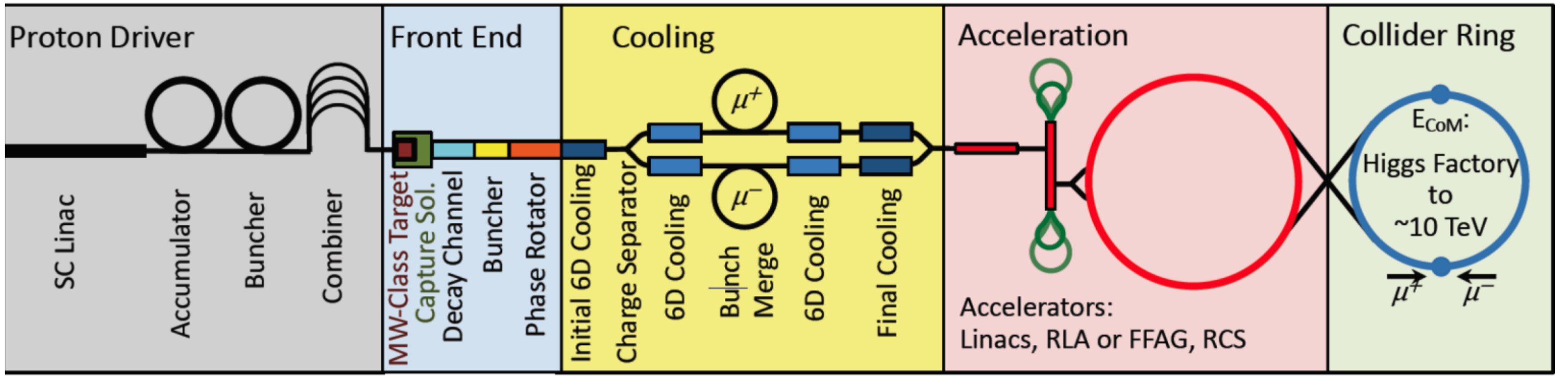

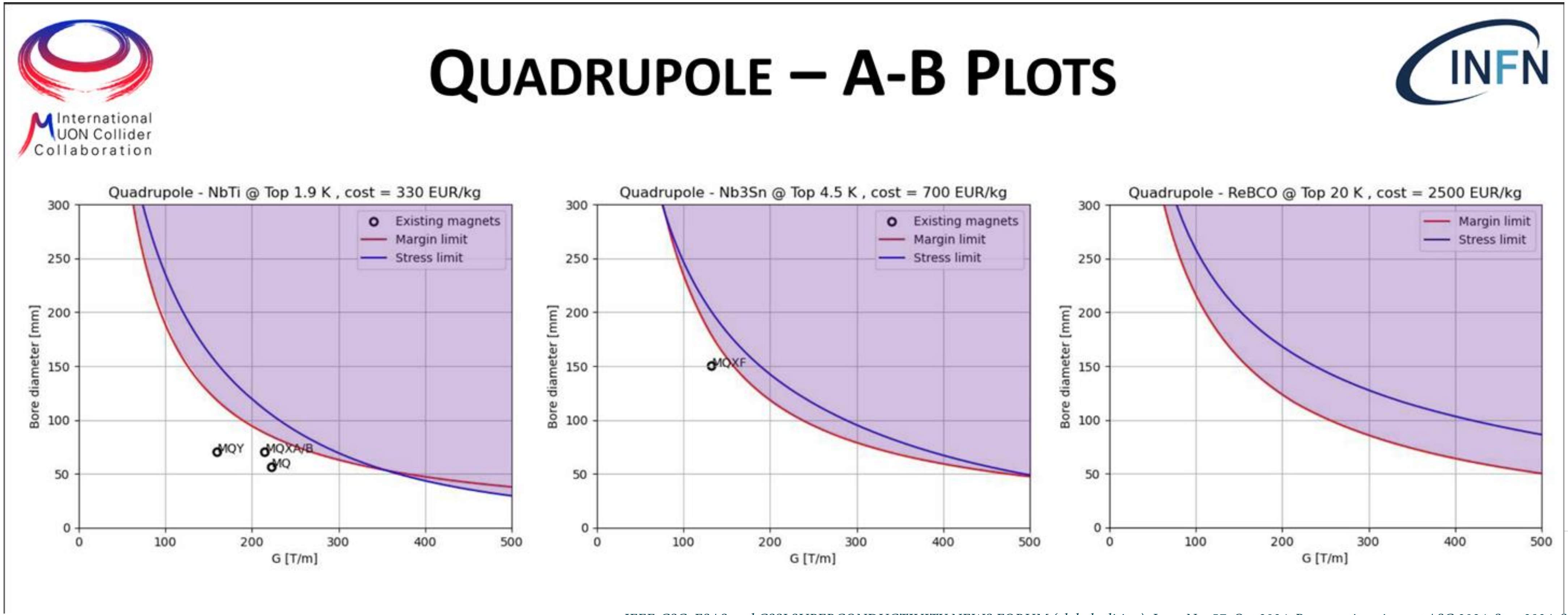

IEEE-CSC, ESAS and CSSJ SUPERCONDUCTIVITY NEWS FORUM (global edition), Issue No. 57, Oct 2024. Presentation given at ASC 2024, Sept 2024, Salt Lake City, Utah, USA.

Fusion

OPEN ACCESS
IOP Publishing | International Atomic Energy Agency
Nuclear Fusion
Nucl. Fusion 64 (2024) 036025 (12pp)
https://doi.org/10.1088/1741-4326/ad2425

Relationship between magnetic field and tokamak size—a system engineering perspective and implications to fusion development

G. Federici[1,2,*], M. Siccinio[1,3], C. Bachmann[1], L. Giannini[1], C. Luongo[1] and M. Lungaroni[4]

Higher field is better? --- or is there an optimum?

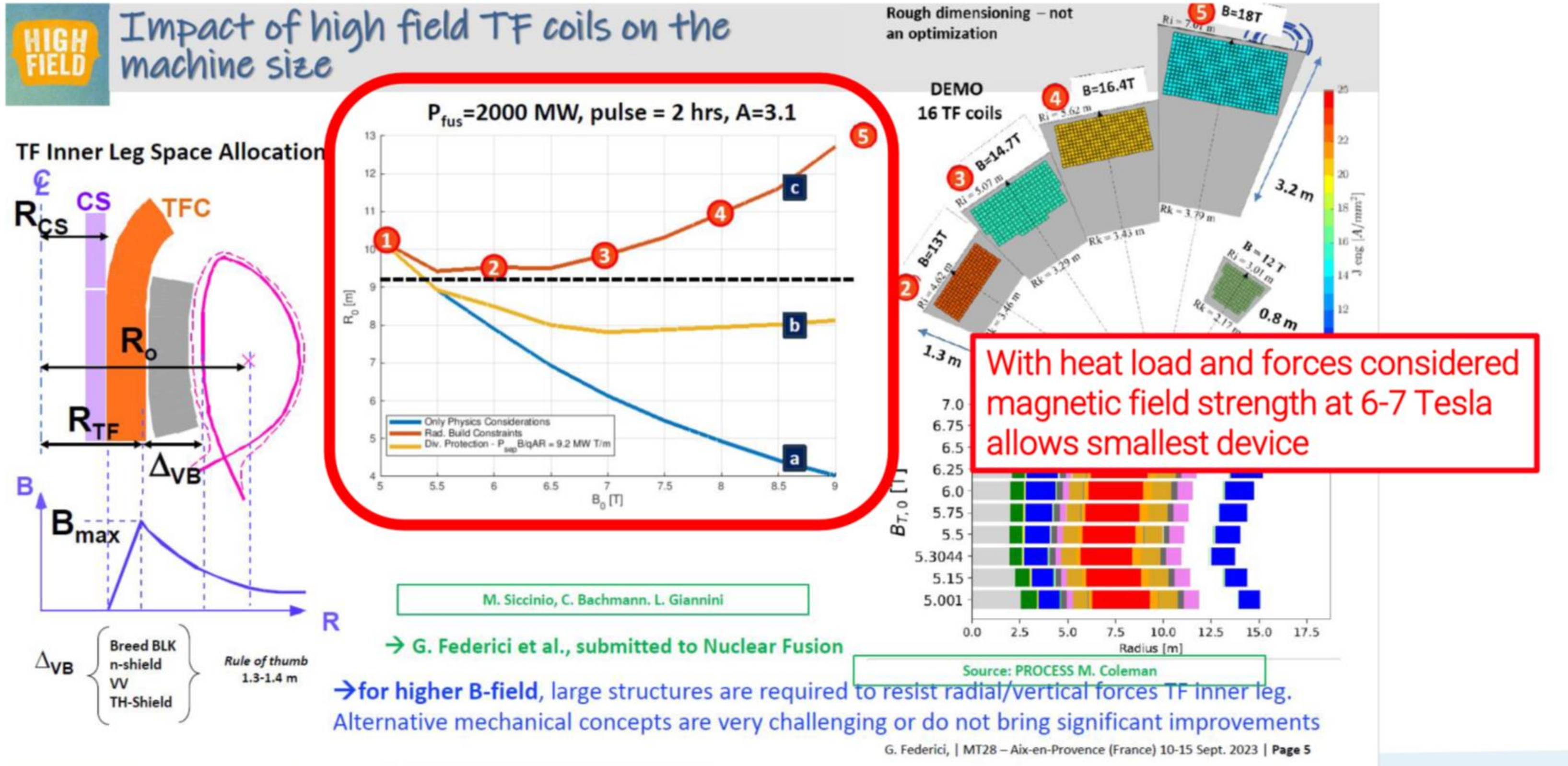

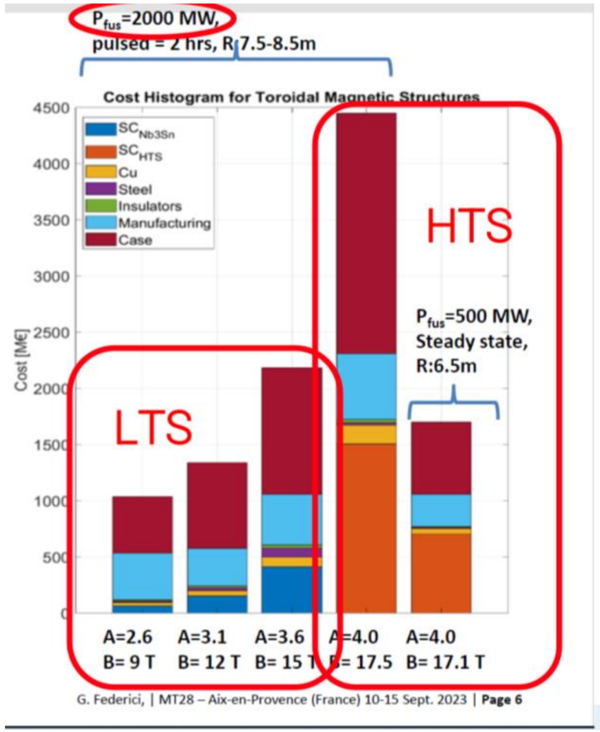

Not exactly Nb-Based: Chevrels?

Prospects of an alternative superconductor technology for fusion reactors

Cite as: Phys. Plasmas **30**, 120604 (2023); doi: 10.1063/5.0162284
Submitted: 14 June 2023 · Accepted: 3 December 2023 ·
Published Online: 20 December 2023

View Online Export Citation CrossMark

B. Seeber[a)]

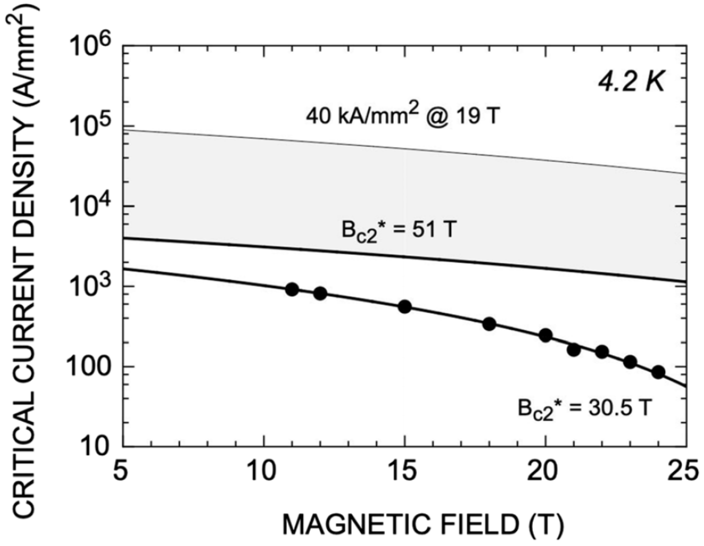

FIG. 6. Critical current density in the superconducting section of a monofilamentary TMC conductor vs magnetic field.[40] The effective upper critical field, estimated by applying a scaling law for the pinning force[41] and extrapolation to zero, is 30.5 T (4.2 K). Increasing the effective upper critical field to 51 T, which means transparent grain boundary behavior, improves substantially the critical current density. The upper limit corresponds to the benchmark critical current density of 40 kA/mm^2 at 19 T/4.2 K.

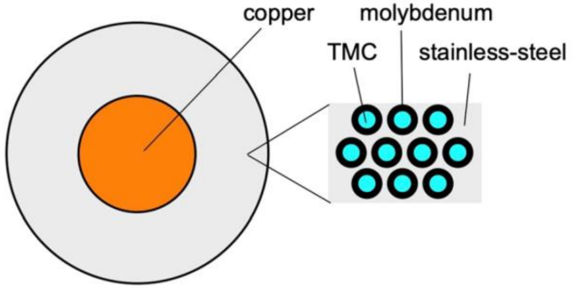

FIG. 2. Schematic layout (not in scale) of a multifilamentary TMC conductor. TMC filaments with a molybdenum diffusion barrier are imbedded in a stainless-steel matrix and stabilization is assured by the copper core.

TABLE III. Constituents of a 0.82 mm TMC wire with 1920 filaments (OD = 10 μm) and a stabilizer/superconductor fraction of 1.

Constituents	Volume (%)	Density (g/cm^3)	Weight (%)
TMC superconductor (PMS)	28.6	6.15	22.5
Mo barrier (stabilizer)	14.3	10.3	18.6
Stainless-steel matrix	42.8	7.8	42.7
Copper (stabilizer)	14.3	8.9	16.2

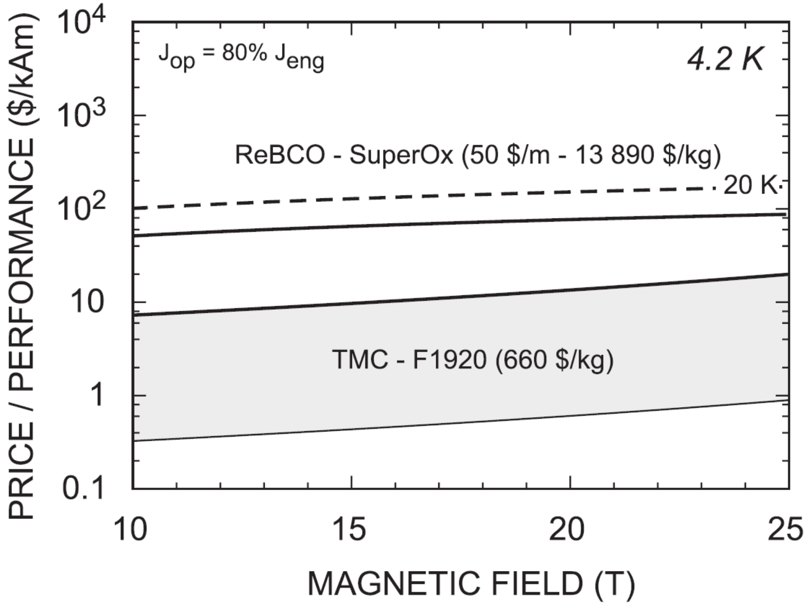

FIG. 4. $/kA m index at 4.2 K vs magnetic field for a TMC multifilamentary wire F1920 is shown with an operating current density of 80% of the engineering current density and a conductor price of 660 $/kg (production scaling factor P = 10). The upper line is the expected behavior for transparent grain boundaries and the lower line corresponds the upper bound estimate for the critical current density (40 kA/mm^2 at 19 T/4.2 K). For comparison, a 4 mm ReBCO tape, manufactured by SuperOx, with a conductor price of 50 $/m (13 890 $/kg) is depicted.

Nb_3Sn undulator for the Advanced Photon source (APS)

Slides Courtesy Ibrahim Kesgin

- A 3-year project supported by the DOE.
- Collaboration among three US National Labs:
  - ANL (lead institution),
  - FNAL (heat treatment & help with the magnet design),
  - LBNL (protection system).
- Project breakdown:
  - R&D Phase: Build and test short prototypes and scaled to a 0.5-meter lengths.
  - Construct a full-scale magnet (1.1 meters long).
  - Modify an existing cryostat to accommodate the Nb_3Sn undulator magnets.
  - Undulator assembly, testing, magnetic characterizations and installation on the APS.

84 mm

~0.5 m long Nb3Sn magnets

Cold mass assembly with the 1.1 m long Nb3Sn magnets

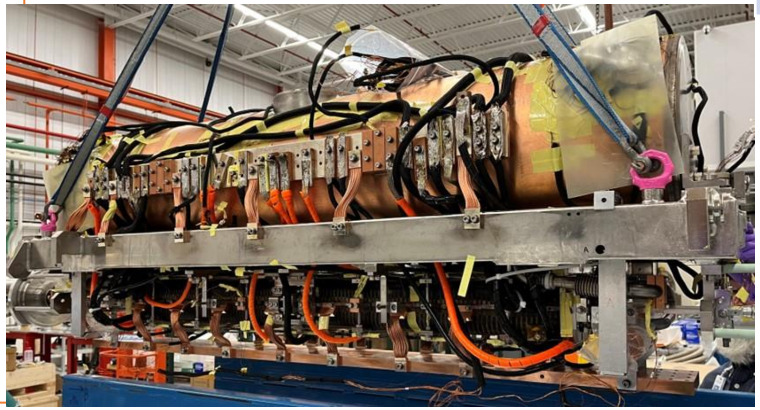

Undulator specifications	Nb_3Sn	NbTi
Undulator Field, T	1.17	0.97
K value	2	1.6
Design current, A (~70 and ~80% of the I_c) at 4.2 K	820	450
Period length, mm	18	18
Magnetic gap, mm	9.5	9.5
Magnetic length, m	1.1	1.1
Vacuum gap, mm	7.2	7.2

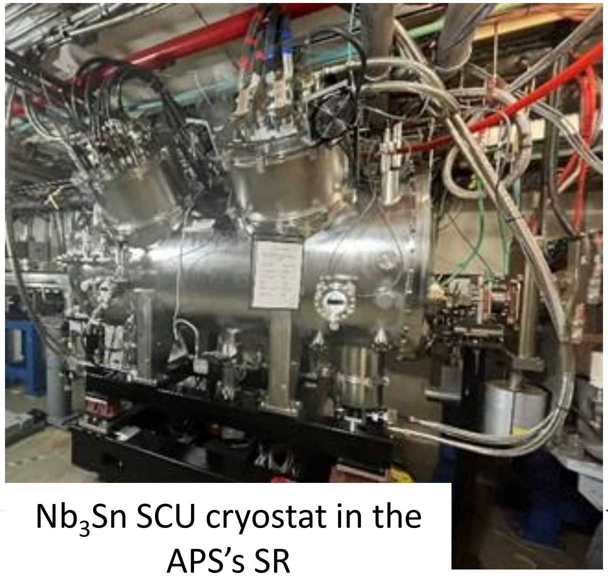

Nb_3Sn SCU cryostat in the APS's SR

Nb_3Sn SCU replaced NbTi SCU in APS's Sector 1 and successfully delivered x-ray beams as the first Nb_3Sn-based SCU. Operated flawlessly until the start of the APS upgrade on April 17th, '23.

I. Kesgin et al., IEEE Transactions on Applied Superconductivity, vol. 34, no. 5, pp. 1-10, Aug. 2024, Art no. 4100905

Undulator quench training and field measurements

Slides Courtesey Ibrahim Kesgin

Vertical test set-up

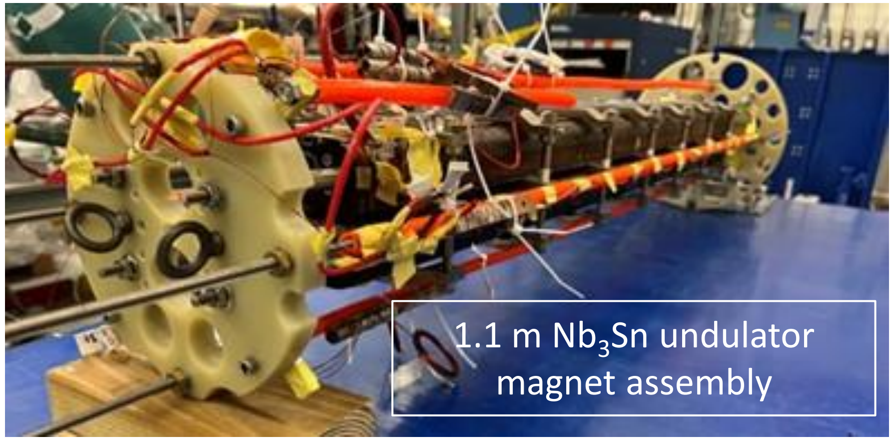

- 1.1m SCU magnets assembled in undulator configuration with diagnostic elements and quench trained
- Undulator achieved design field without requiring additional training during the second cooldown
- **Phase error of <6 degrees achieved up to the maximum operating current**

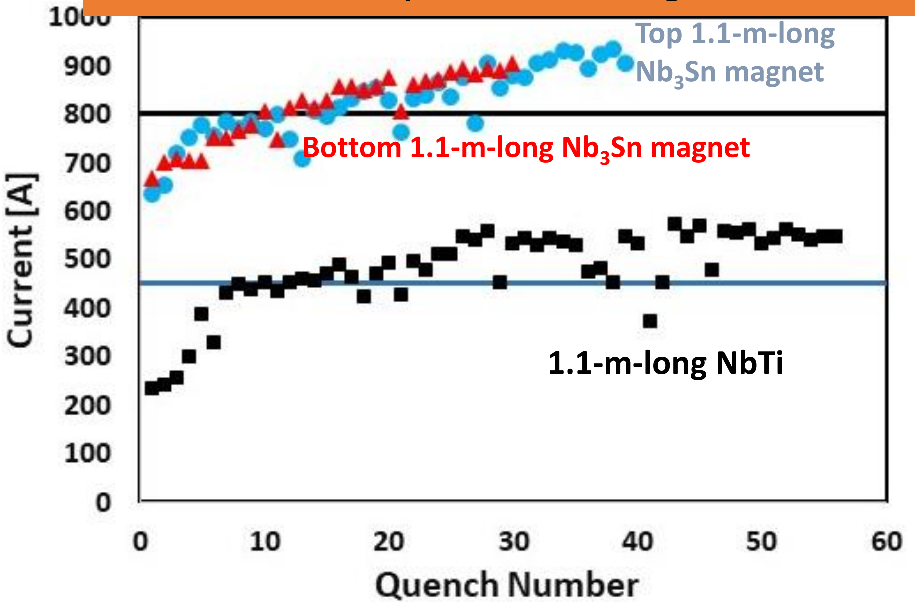

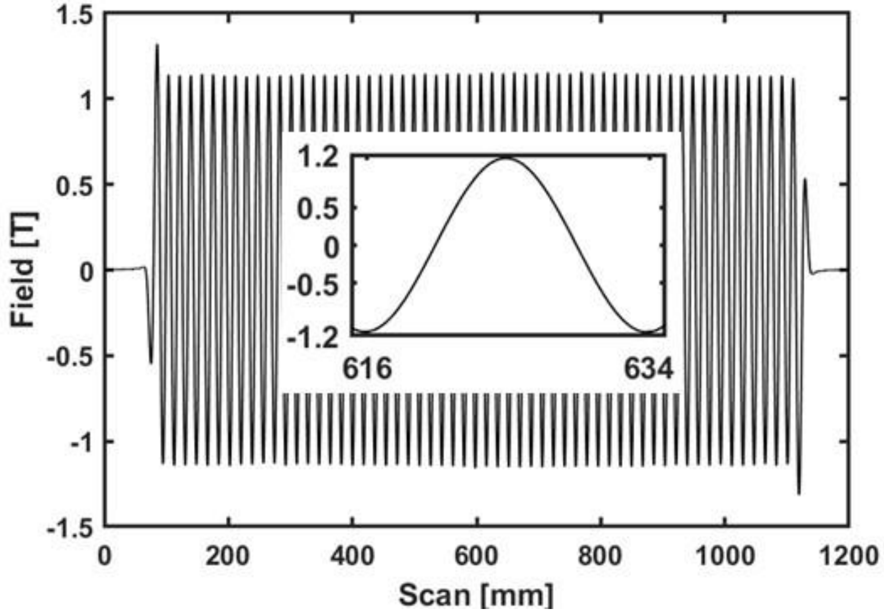

Work supported by the U.S. Department of Energy, Office of Science, under Contract No. DE-AC02-06CH11357
Through Accelerator & Detector Research Program

IEEE-CSC, ESAS and CSSJ SUPERCONDUCTIVITY NEWS FORUM (global edition), Issue No. 57, Oct 2024. Presentation given at ASC 2024, Sept 2024, Salt Lake City, Utah, USA.

Nb_3Sn in FCC or FCC-like accelerator magnets

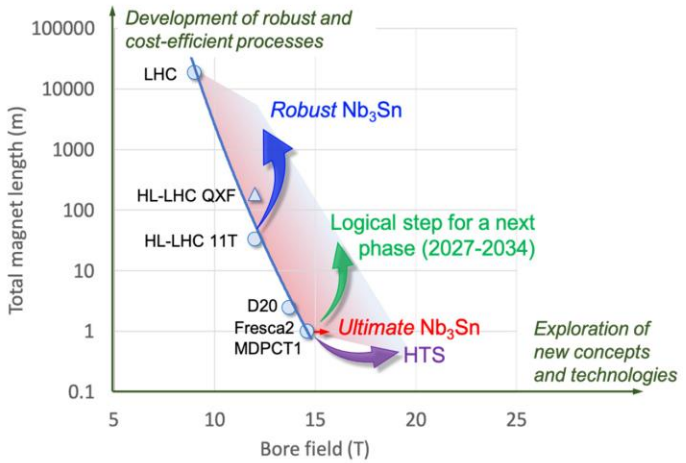

Fig. 3. Graphical representation of the objective of the HFM R&D program in this phase, 2021-2027. Both fronts of maximum field (red for Nb_3Sn, purple for HTS) and large-scale production (blue) are intended to be advanced at the same time. Also represented, in green, a possible evolution for the longer term, 2027-2034.

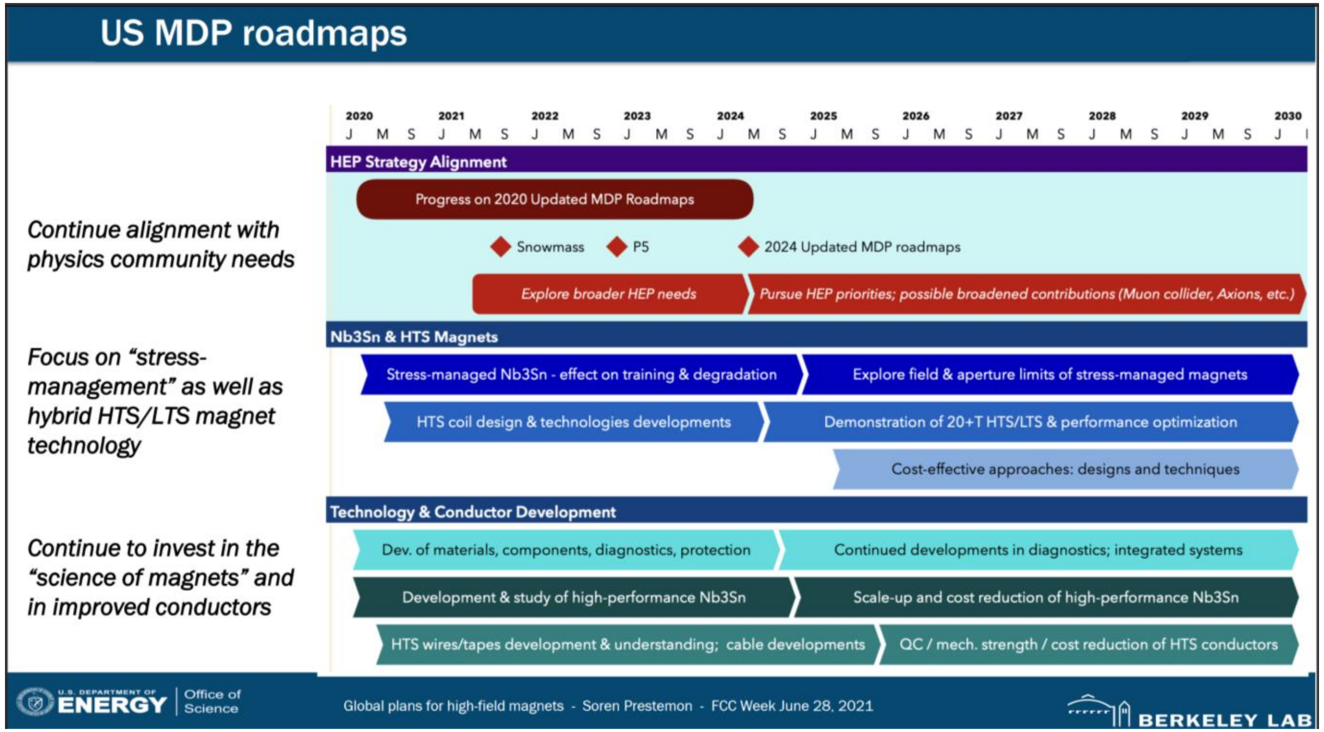

High Field Accelerator Magnets for Next Generation Colliders – Motivation, Goals, Challenges and R&D Drivers

https://doi.org/10.1142/9789811278952_0031

FERMILAB-TM-2807-TD

CONCEPTUAL DESIGN OF A 20 T DIPOLE BASED ON HYBRID REBCO/Nb_3Sn COS-THETA COIL*

A. V. Zlobin†, Fermilab, Batavia, IL 60510, USA

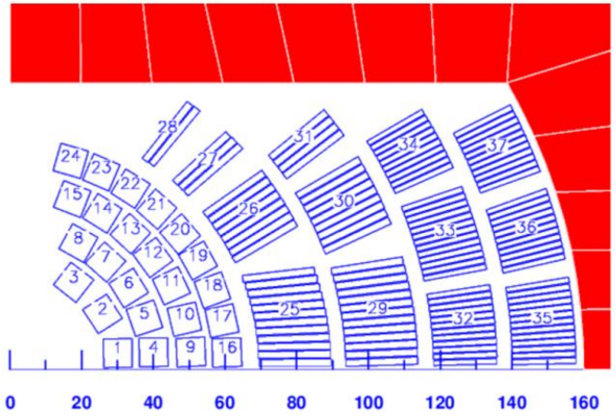

Figure 3: Cross-section of one quadrant of the 20 T hybrid REBCO/Nb_3Sn dipole coil inside the iron yoke.

Table 3: Magnet Parameters

Parameter	REBCO/ Nb_3Sn	Bi2212/ Nb_3Sn
Nominal current I_{nom}, kA	14.90	13.45
Nominal bore field B_o, T	20.0	20.0
Coil nominal field B_{nom}, T	20.34	20.04
Magnet $TF=B_o/I_{nom}$ at I_{nom}, T/kA	1.342	1.487
Magnet margin at 1.9 K, %	10.9	13.2
Total HTS coil area, mm^2	601	972
Total Nb_3Sn coil area, mm^2	3854	3110
Total coil area, mm^2	4455	4082

Novel Developments in Nb_3Sn and Nb_3Al

- Very fine wires and cables (NIMS and commercial collaborators) of Nb_3Sn and Nb_3Al (NIMS)

- Progress in APC conductors

- Possible Progress in Nb_3Sn *Bc2*

IEEE-CSC, ESAS and CSSJ SUPERCONDUCTIVITY NEWS FORUM (global edition), Issue No. 57, Oct 2024. Presentation given at ASC 2024, Sept 2024, Salt Lake City, Utah, USA.

Development at NIMS (Courtesy of A. Kikuchi)

10 microns Nb_3Al Jelly-Rolled Mono-Core Wire

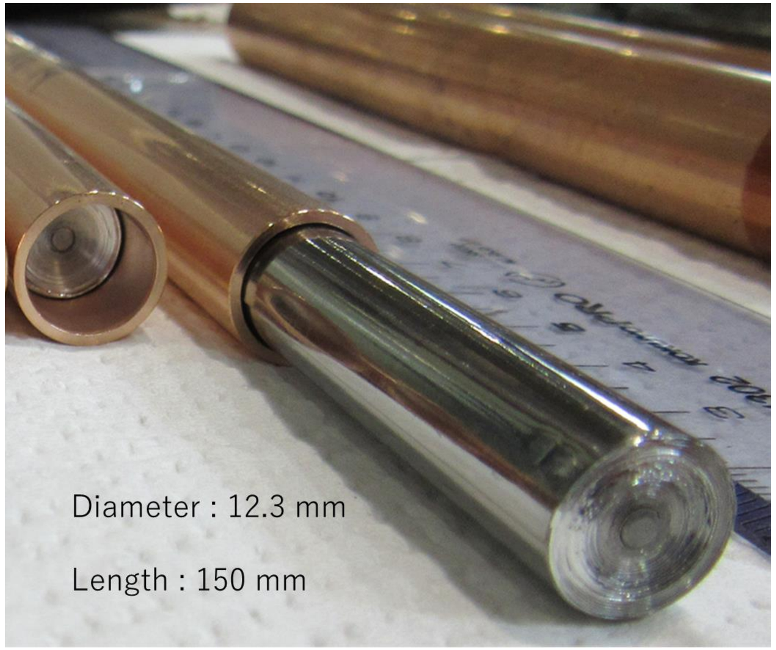

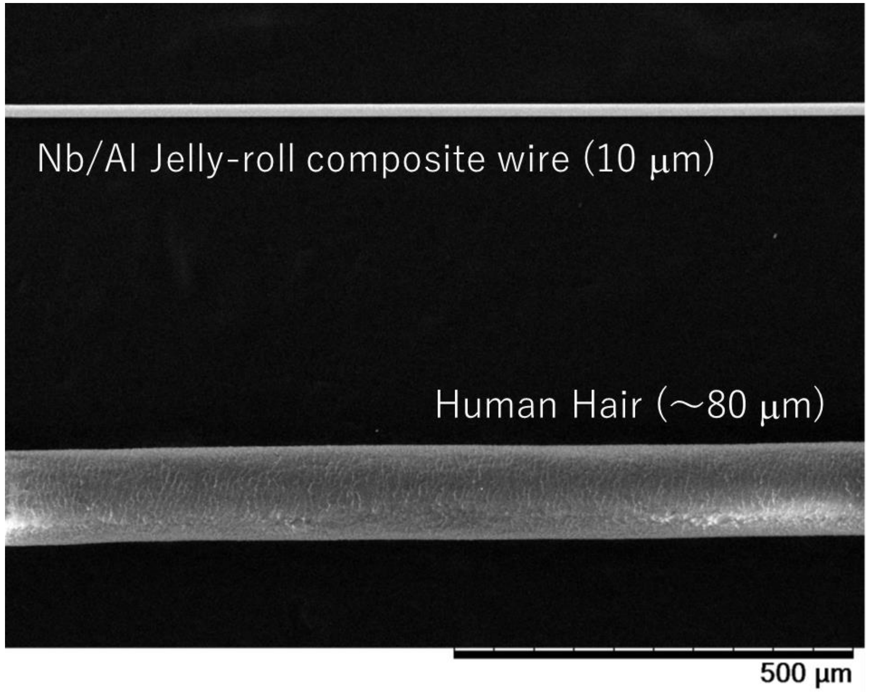

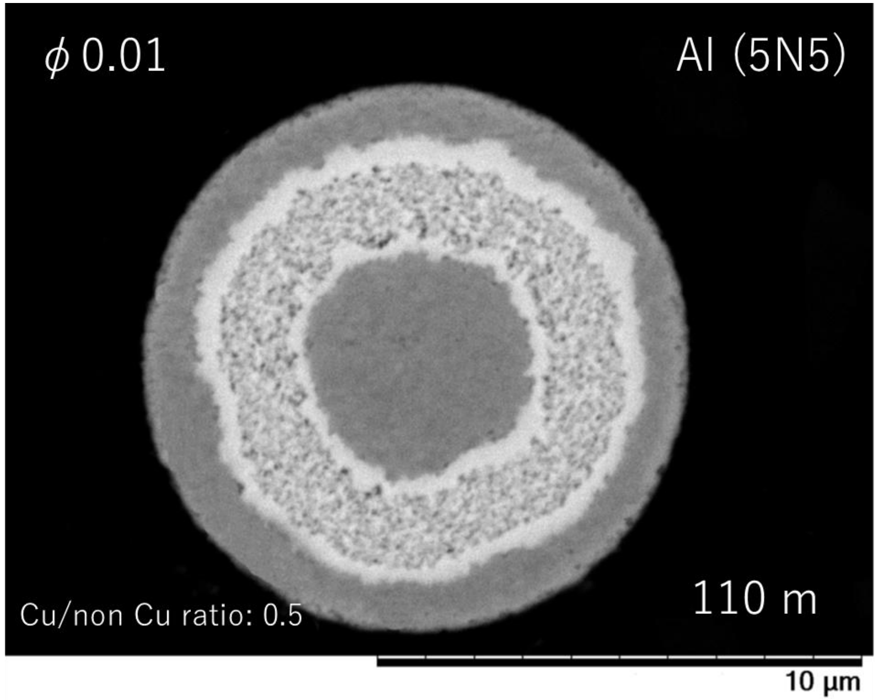

The thinnest Nb_3Al superconducting wire in the world!

IEEE-CSC, ESAS and CSSJ SUPERCONDUCTIVITY NEWS FORUM (global edition), Issue No. 57, Oct 2024. Presentation given at ASC 2024, Sept 2024, Salt Lake City, Utah, USA.

50 microns Bronze-Processed Nb_3Sn Multifilamentary Wires

Development at NIMS (Courtesy of A. Kikuchi)

Mass-Production Scale
50 microns Nb_3Sn Ultrafine Wires

(a) Cu13.5Sn0.3Ti (Billet # : SS153) (b) Cu14.6Sn0.3Ti (Billet # : SK268) (c) Cu16Sn0.3Ti (Billet # : SK262)

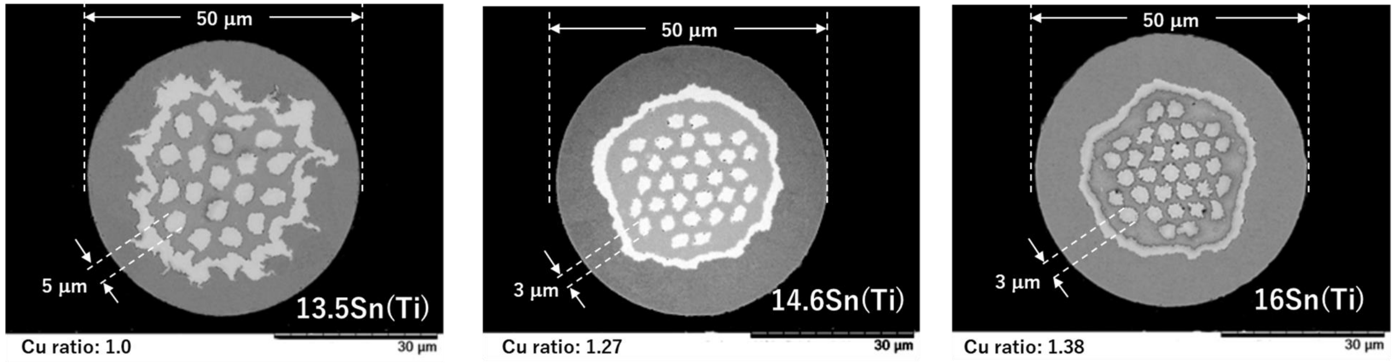

8 inches Billet

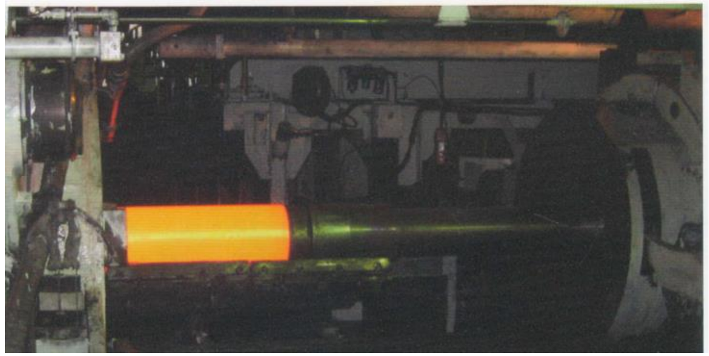

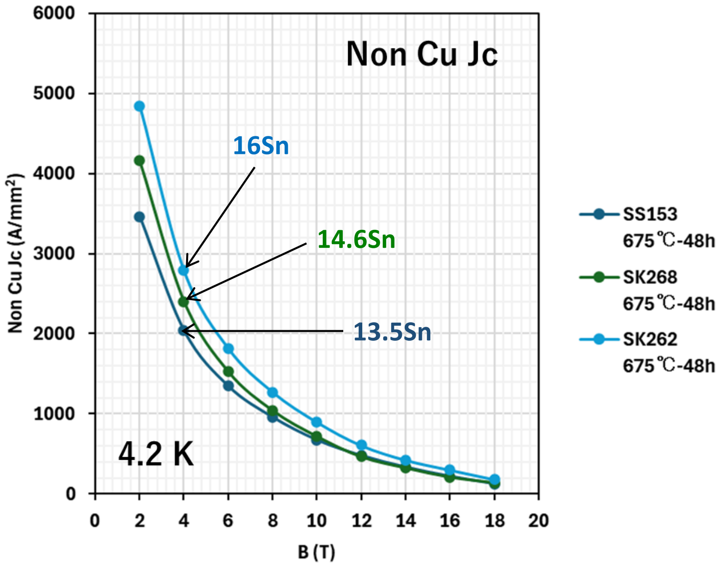

Demonstration of Large Current Capacity
Flexible Nb_3Sn Conductor

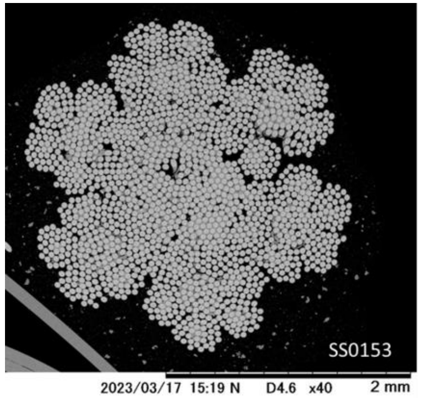

(a) Transport Ic (A)

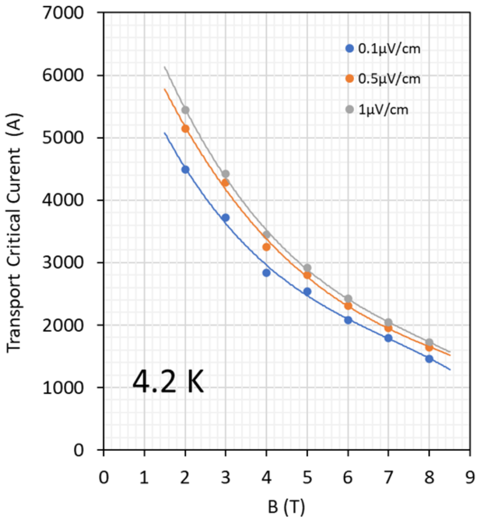

(b) Overall Jc (Je) (A/mm²)

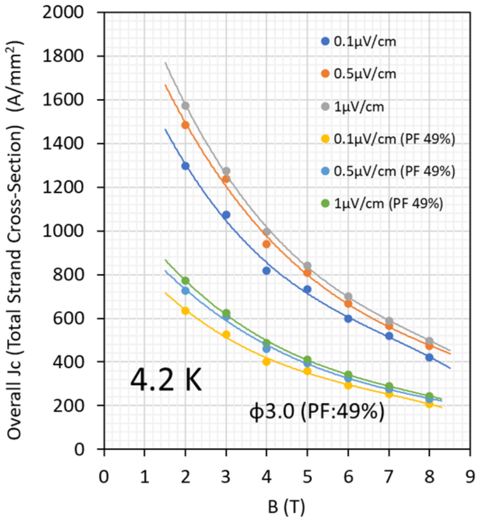

50 microns Jelly-Rolled Nb_3Sn Mono-Core Wire

Development at NIMS (Courtesy of A. Kikuchi)

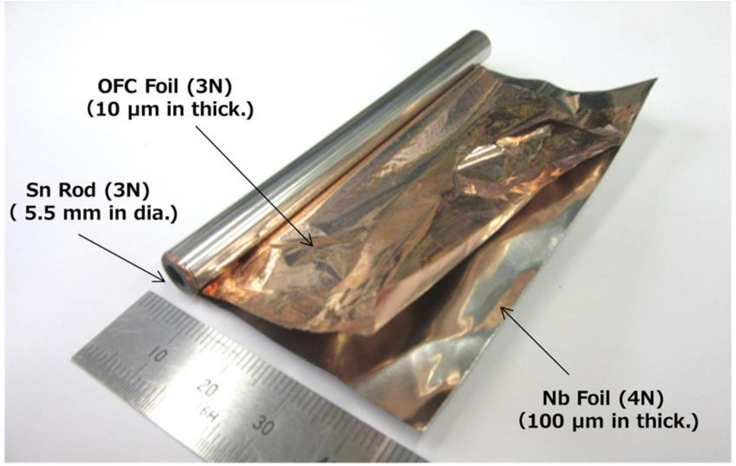

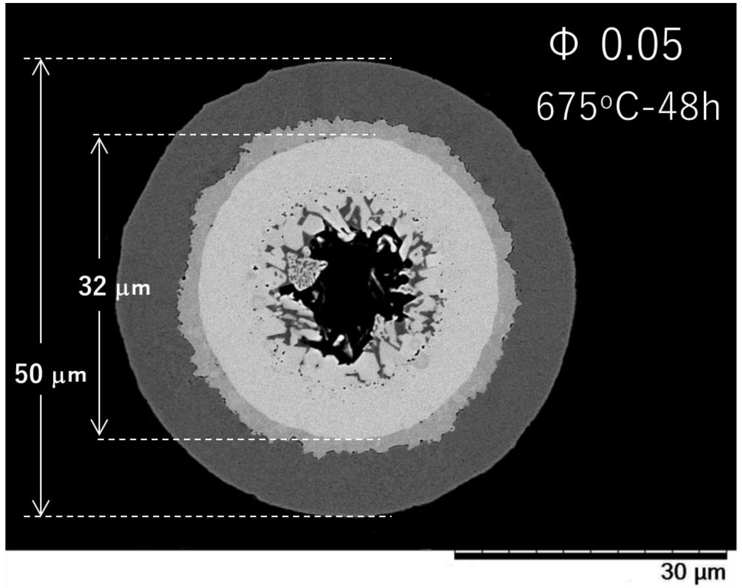

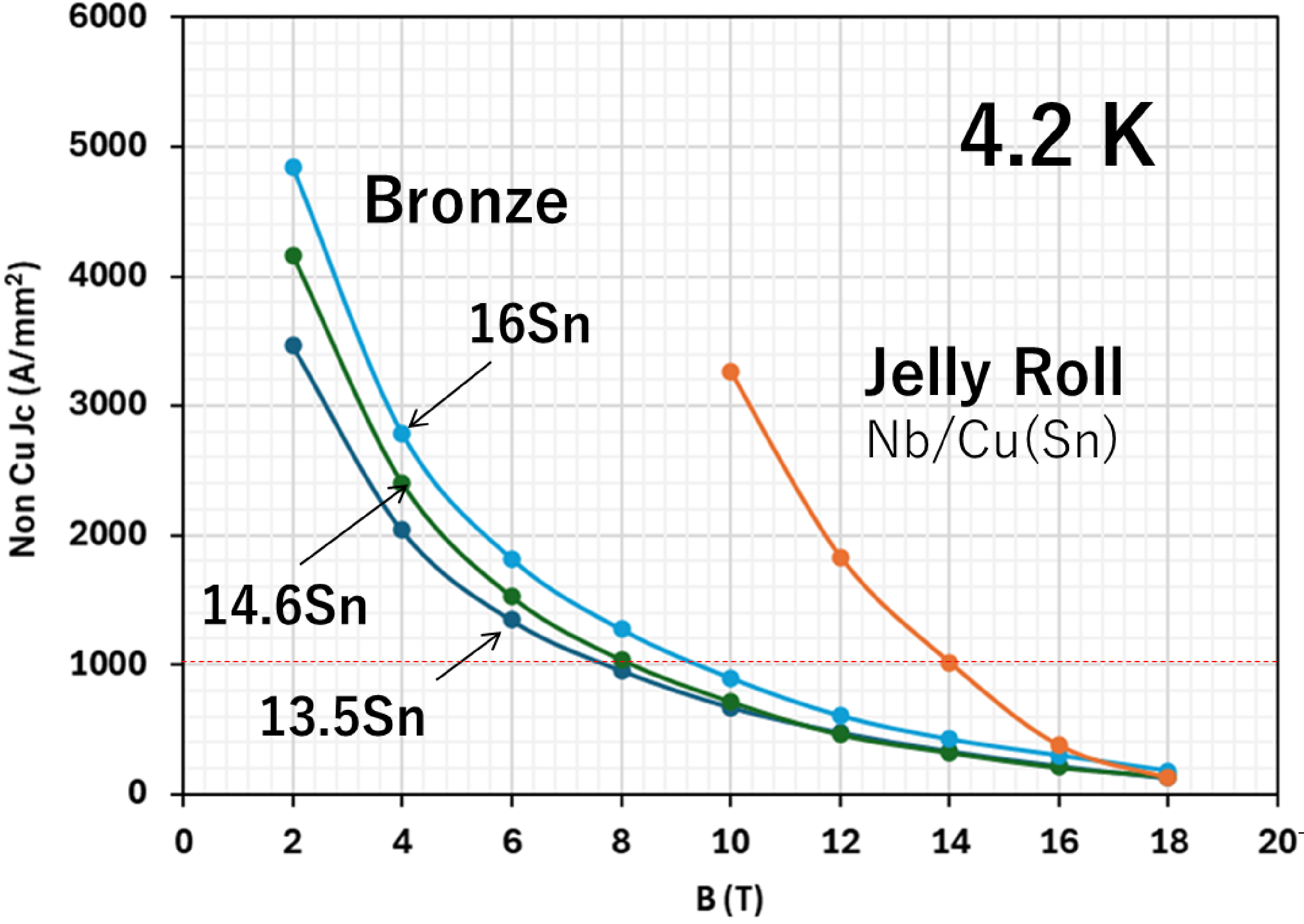

IEEE-CSC, ESAS and CSSJ SUPERCONDUCTIVITY NEWS FORUM (global edition), Issue No. 57, Oct 2024. Presentation given at ASC 2024, Sept 2024, Salt Lake City, Utah, USA.

Nb_3Sn Challenges and Opportunities

- New frontiers in performance!
- Increase J_c, J_e
- Increase B_{c2}
- Increase Stability as J_{c2} and B_{c2} go up
- High quality, long length, commercial manufacture
- Development of commercial products for continuity

IEEE-CSC, ESAS and CSSJ SUPERCONDUCTIVITY NEWS FORUM (global edition), Issue No. 57, Oct 2024. Presentation given at ASC 2024, Sept 2024, Salt Lake City, Utah, USA.

Well, What are the flux Pinning sites in Nb_3Sn? - Grain Boundaries!- Can we get more of them?

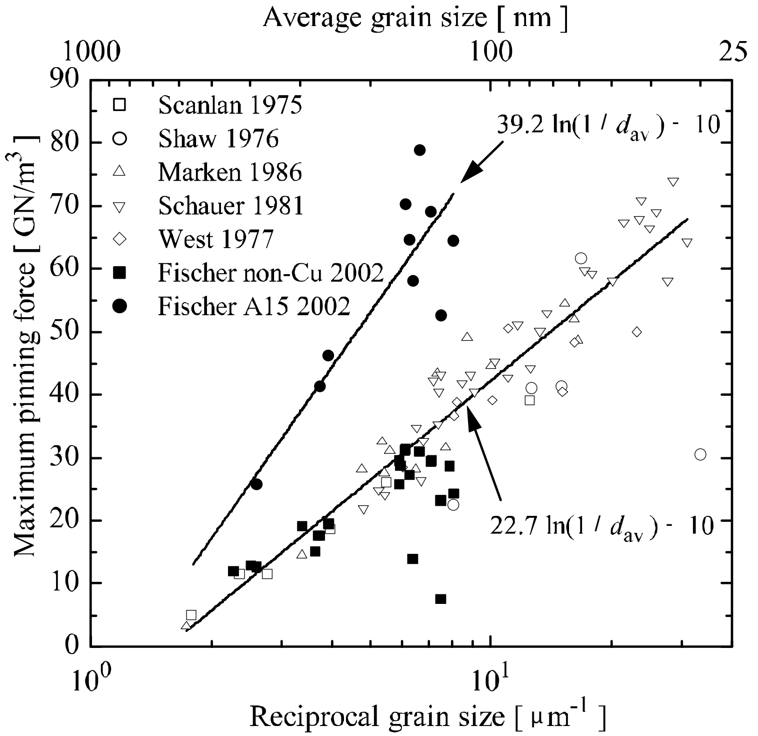

We could add more Surface pins (refine GBs)

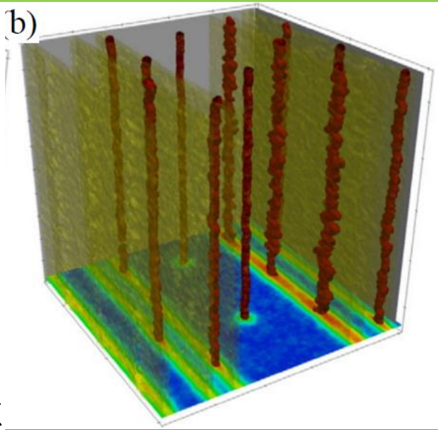

Kwok

Or, could we add Point pins?

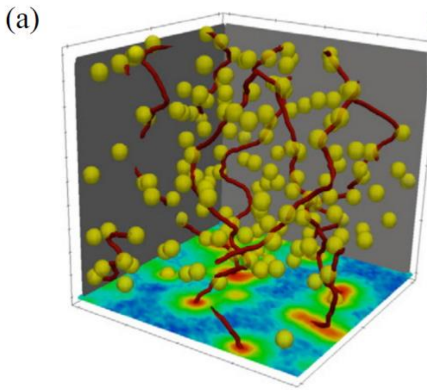

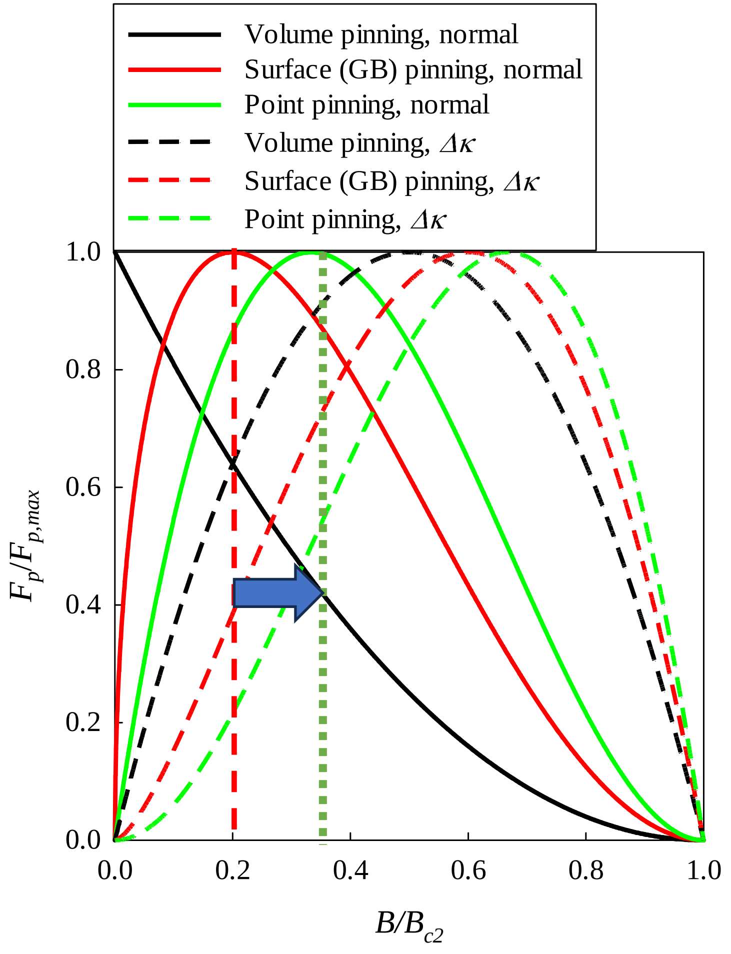

Dew Hughes

- F_{pmax} (4.2 K) vs inverse grain size for Nb_3Sn.
- Compilation by Fischer.
- Pinning force scales as 1/GB size

But, not only GB refinement (via Zener Pinning) - also Direct Fluxon pinning

FNAL-HTR-OSU

GBs show precipitates (slows their growth and thus “refines” them)

Pins inside grains -- directly pin flux also

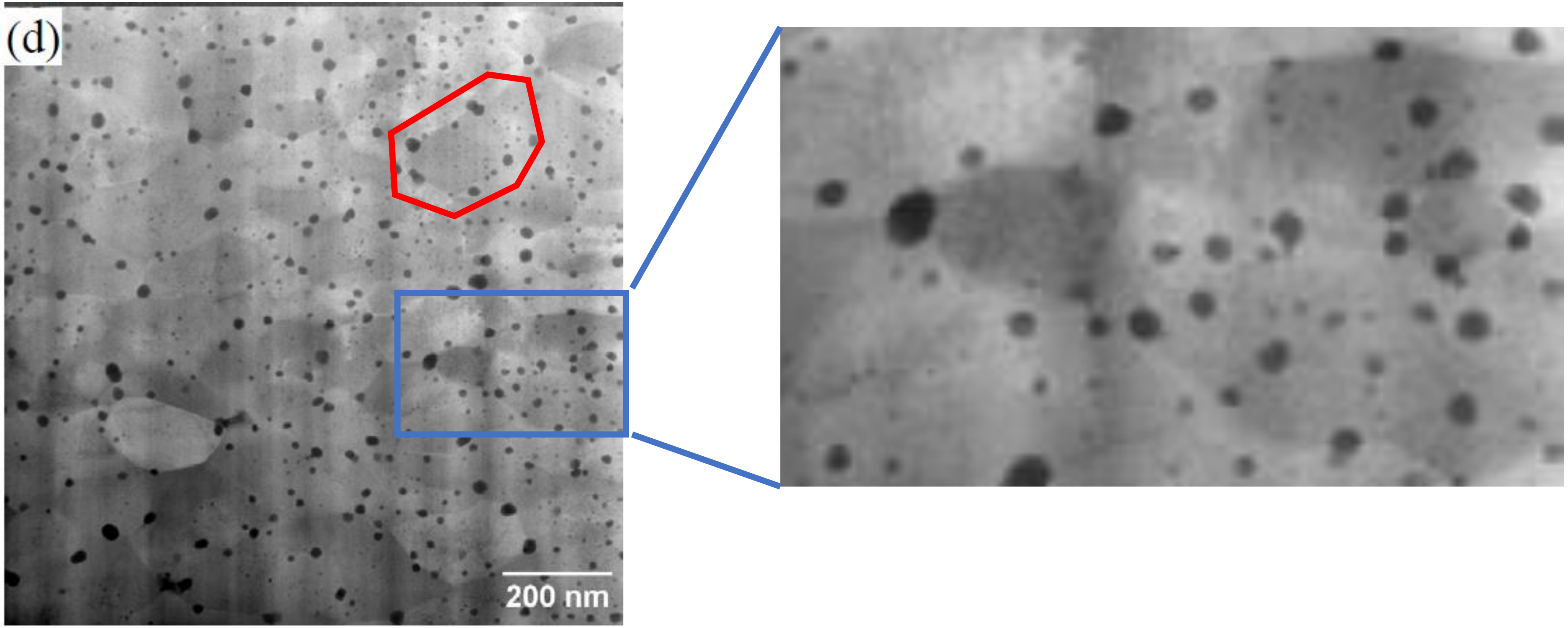

IEEE-CSC, ESAS and CSSJ SUPERCONDUCTIVITY NEWS FORUM (global edition), Issue No. 57, Oct 2024. Presentation given at ASC 2024, Sept 2024, Salt Lake City, Utah, USA.

FG/CG ratios of APC Nb_3Sn conductors based on Nb-Ta-Hf/Zr

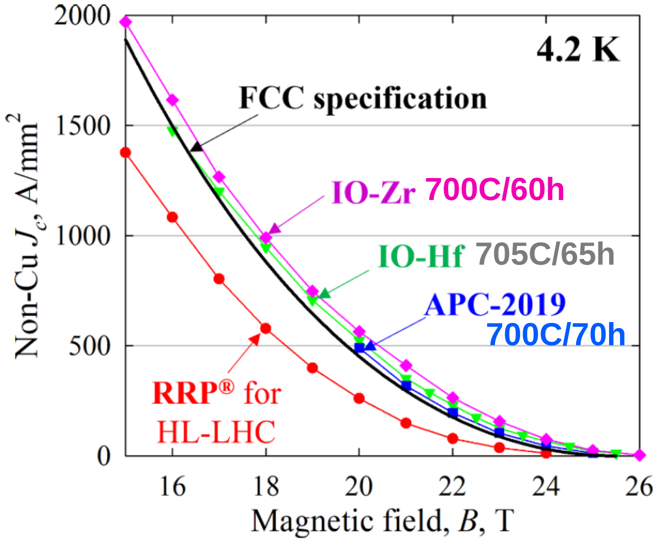

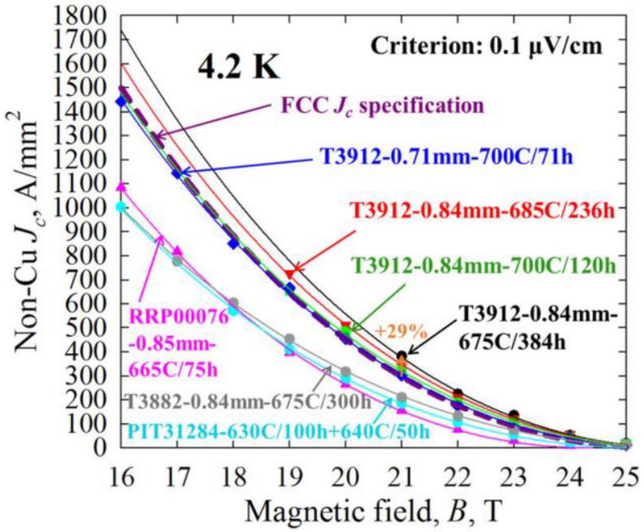

In previous works:

- Most APC Nb_3Sn conductors which surpassed the level of FCC specification were reacted at ~ 700 ^oC due to high FG/CG ratio and small grain-size.
- The APC Nb_3Sn conductor reacted at 675 ^oC attained the highest non-Cu J_cs due to even smaller grain size, but low stability

X Xu et al 2023 *Supercond. Sci. Technol.* 36 035012

X Xu et al 2019 arXiv:1903.08121

Sample	H.T. (^oC x h)	FG/CG
APC-1.0%Hf	675 x 400	1.81
	685 x 248	1.91
	705 x 85	2.37
APC-1.0%Zr	675 x 270	1.63
	685 x 125	2.19
	700 x 62	2.61
PIT-standard	630 x 100 + 640 x 50	3.08

- For achieving high non-Cu J_cs, the APC wire reacted at 675 ^oC needs to have very aggressive recipe due to low FG/CG ratio, inducing low stability.
- If we increase FG/CG ratio at heating temperature ≤ 675 ^oC, we can use more conservative recipe for APC wire.
- It is expected that APC wires reacted at low heating temperature simultaneously achieve high non-Cu J_c and stability

IEEE-CSC, ESAS and CSSJ SUPERCONDUCTIVITY NEWS FORUM (global edition), Issue No. 57, Oct 2024. Presentation given at ASC 2024, Sept 2024, Salt Lake City, Utah, USA.

(2-4) Solubility drop → concentration spike at interface

2. **<u>Solubility Difference:</u>** Scarce literature on Nb_3Sn solubility suggests:
    - Zr solubility in Nb_3Sn ~ 1-4.3% [1, 2]
    - O solubility in Nb_3Sn ~ 0.4-0.5% [2, 3]
3. **<u>Pile up at moving interface:</u>**

    Atom-probe tomography [4] shows that as Nb_3Sn forms, Zr & O pushed ahead of Nb_3Sn/Nb interface
4. **<u>Excess Zr+O drives nucleation:</u>**

    Concentration spike drives nucleation at the interface

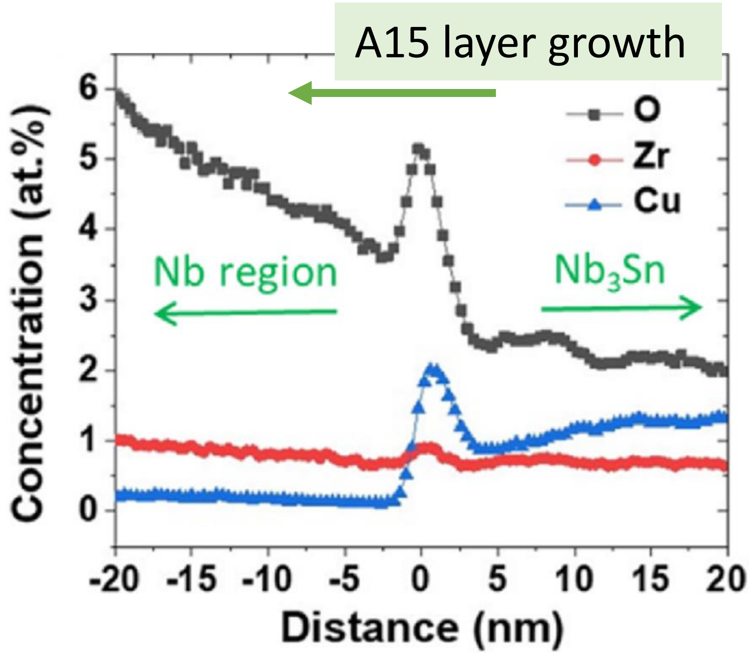

(b)

Atom-probe results from Jae-Yel Lee

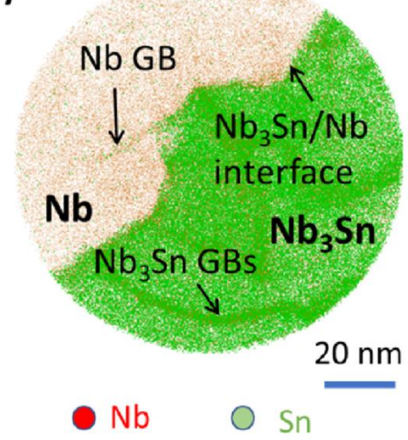

[1] D. Sharma, D. Kalyan, S. K. Makineni, and S. Santra, *Journal of Alloys and Compounds*, vol. 935, p. 168140, 2023.
[2] I. V. Efimov, B. P. Mikhailov, and E. A. Moroz, *Izvestiia Akademii nauk SSSR. Metally.*, pp. 168–172, 1979.
[3] D. B. Smathers and D. C. Larbalestier, in *Filamentary A15 Superconductors*, M. Suenaga and A. F. Clark, Eds. Boston, MA: Springer US, pp. 143–154, 1980.
[4] Atom-probe results from Jae-Yel Lee, published in X. Xu, M. D. Sumption, J. Lee, J. Rochester, and X. Peng, *J. Alloys Compounds*, Art. no. 156182, 2020.

Starting size of precipitate dictated by thermodynamics

- Applies not just to ZrO_2 but also HfO_2 (and TiO_2)
- Different oxides have different Gibbs energies (and precipitate sizes)
- Larger reduction in Gibbs energy → smaller particles can nucleate

$$\Delta G = \frac{4}{3}\pi r^3(\boldsymbol{\Delta g_v} - \Delta g_s) + 4\pi r^2\gamma$$

	Ti	Zr	Hf
d, est, nm	6	1.4	1.3
d, meas, nm	50	10	5

Why large disagreement? – one reason Growth!

Ti – Large
Zr – Medium
Hf – Small

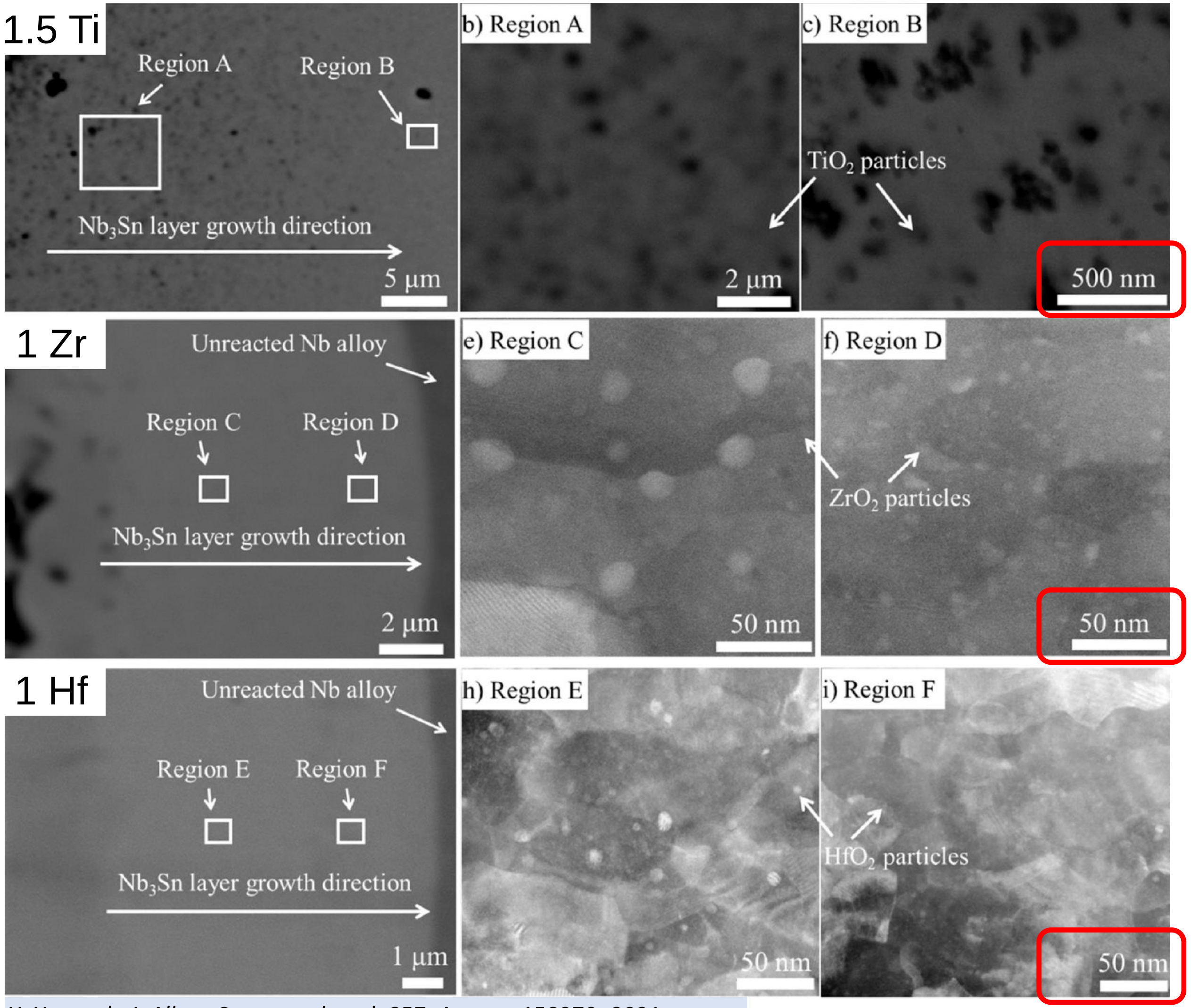

X. Xu *et al.*, *J. Alloys Compounds*, vol. 857, Art. no. 158270, 2021.

(5) Particle Growth Over Time

- **Fine dispersion of particles near interface** (1-2 nm, fewer up to ~10 nm)
- **Coarsen into fewer, larger particles** (up to ~30 nm) **towards core**, or for “longer times”
- Wide particle size distribution – cannot approximate as one size

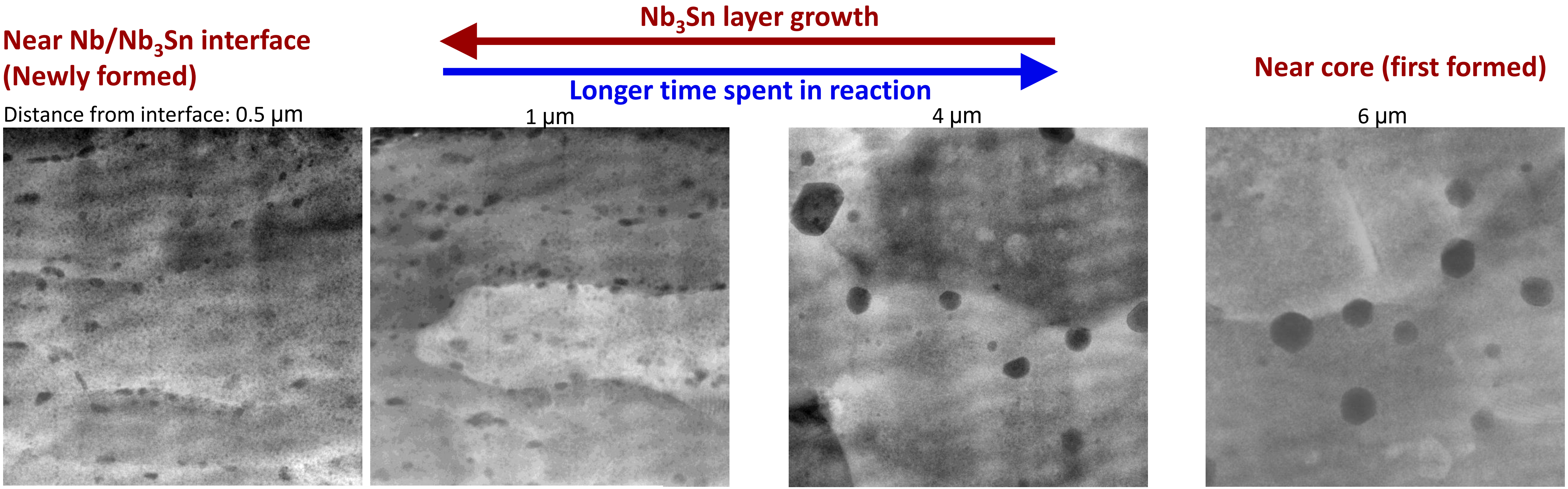

HAADF-STEM images (200 nm x 200 nm) of **Zr APC wire, 720°C/32h**
processed in ImageJ with Gaussian blur and “Enhance Local Contrast” function

IEEE-CSC, ESAS and CSSJ SUPERCONDUCTIVITY NEWS FORUM (global edition), Issue No. 57, Oct 2024. Presentation given at ASC 2024, Sept 2024, Salt Lake City, Utah, USA.

Particle Growth Over Time

- **Zr APC, 740°C/16h**
- The volume-fraction histogram shows the change in size distribution from 2 µm from the Nb/Nb_3Sn interface to 5 µm from the interface
- At distances further from interface, particle coarsening is seen

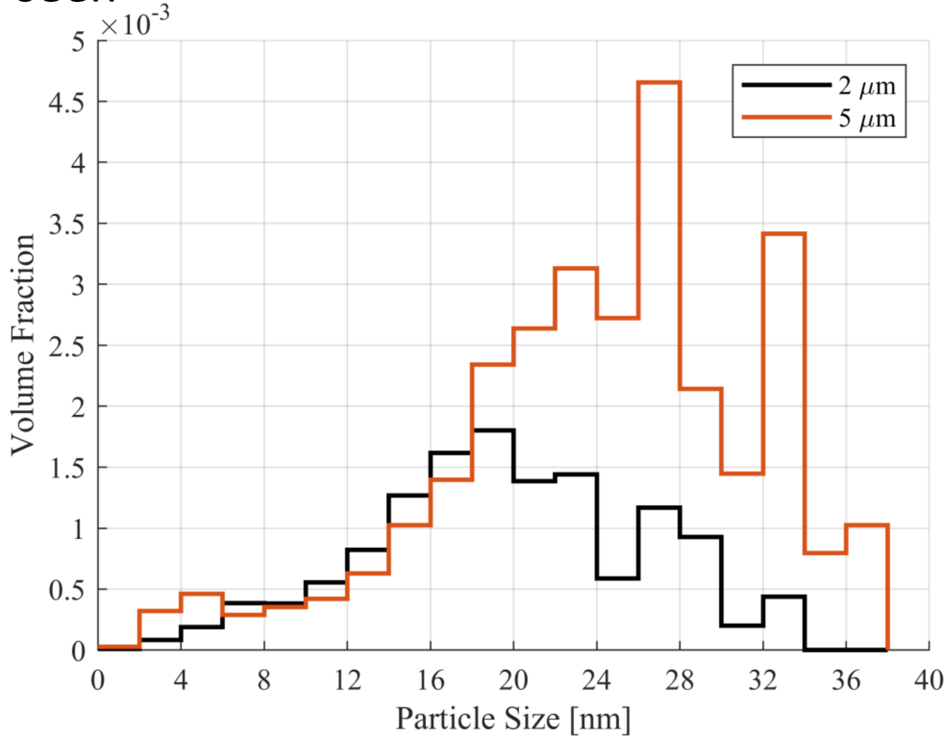

- Distances measured from the reaction interfaces
- Larger distances describe regions that have had longer for particles to coarsen

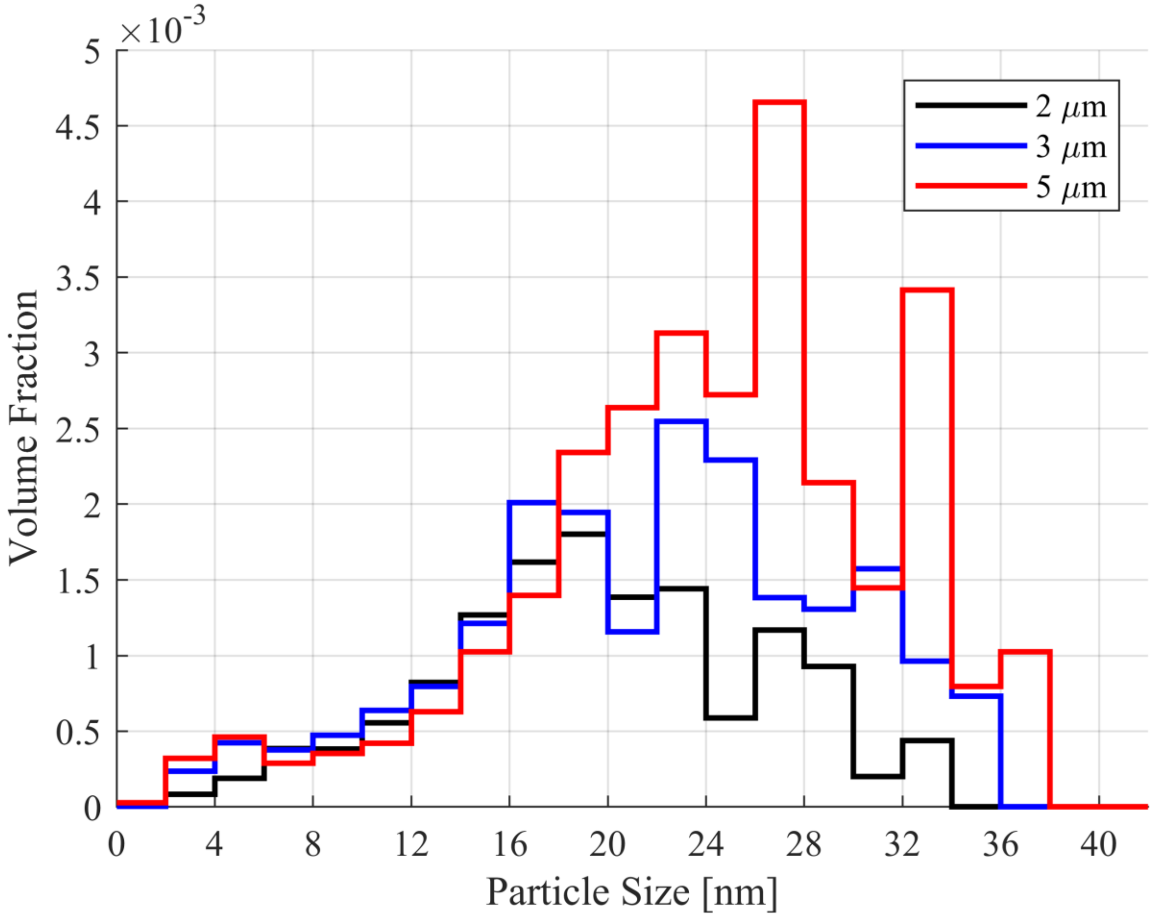

IEEE-CSC, ESAS and CSSJ SUPERCONDUCTIVITY NEWS FORUM (global edition), Issue No. 57, Oct 2024. Presentation given at ASC 2024, Sept 2024, Salt Lake City, Utah, USA.

Number Density of APC at 2μm from Nb/A15 interface

Notice

- Log-normal distribution
- Bimodal distribution

… perhaps larger precipitates are at GBs -- uncertain

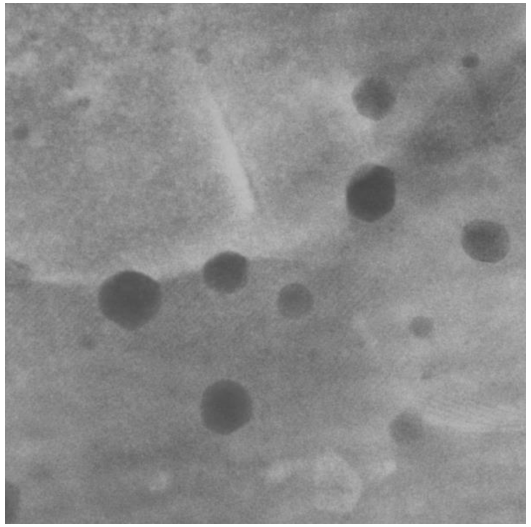

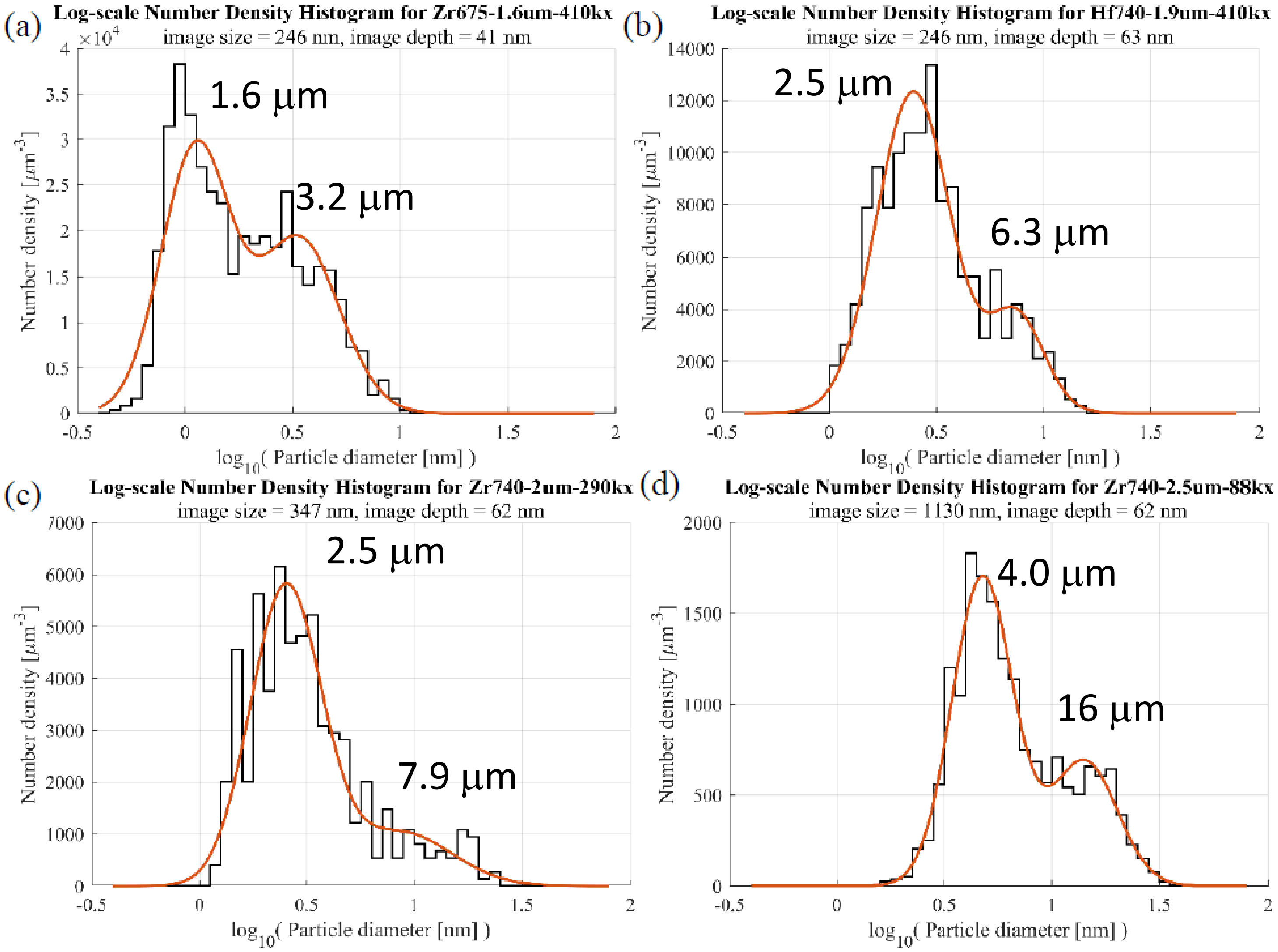

Figure 5.8. Selected particle size distributions from near 2 μm from the Nb/Nb_3Sn interface plotted on a logarithmic axis, from (a) Zr675, (b) Hf740, (c) Zr740 taken at high magnification, and (d) Zr740 taken at low magnification. Curve fit is of a Gaussian mixture model which fits two normal distributions to the data.

Growth of precipitates through the layer (with time)

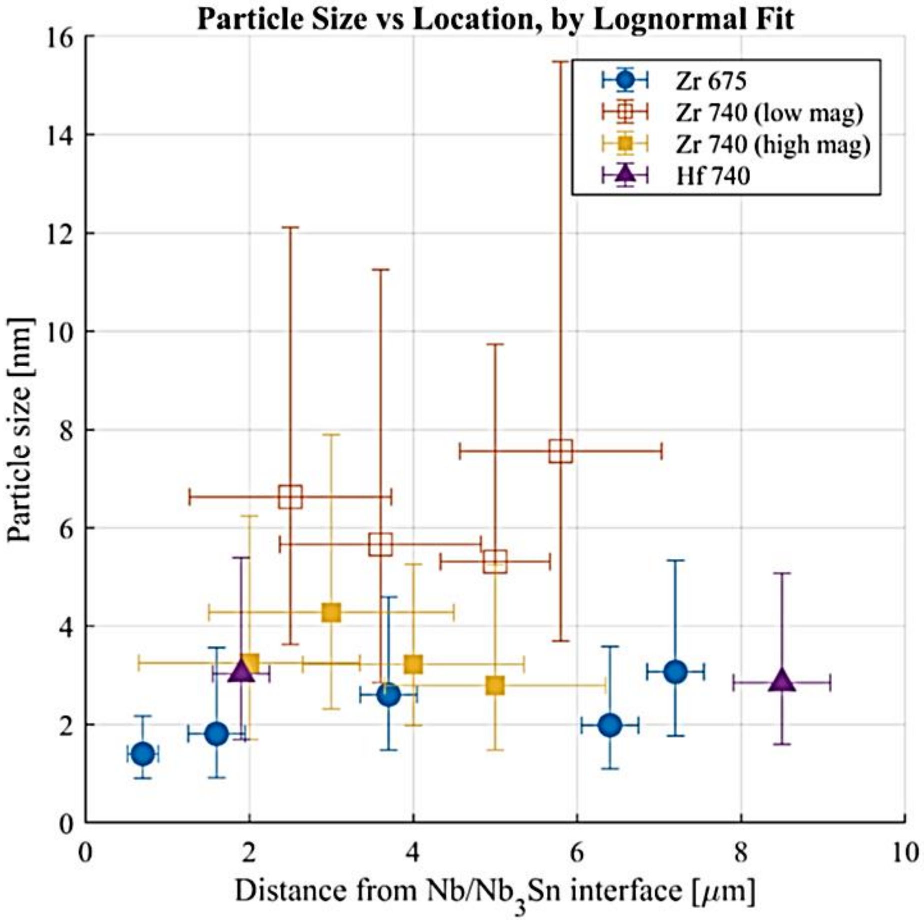

Figure 5.9. Particle size vs distance from the Nb/Nb_3Sn interface based on the lognormal distribution. Points represent the parameter μ and vertical error bars represent the parameter σ (the mean and standard deviation of the logarithms of particle size, respectively). The horizontal error bars represent the sum of the image width and the uncertainty in image location.

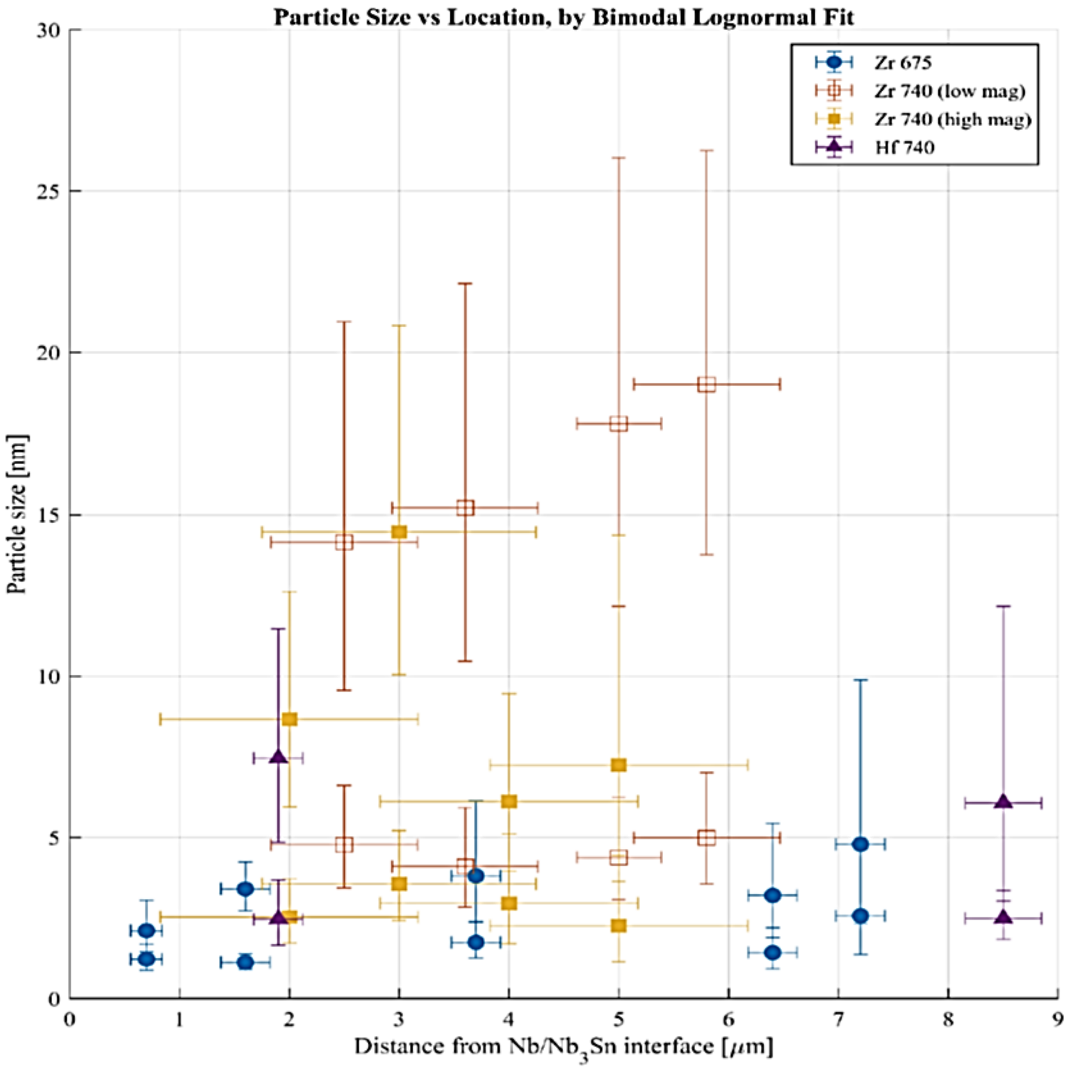

Figure 5.10. Particle size vs distance from the Nb/Nb_3Sn interface based on the bimodal lognormal distribution. Points represent the parameter μ and vertical error bars represent the parameter σ (the mean and standard deviation of the logarithms of particle size from both peaks in the bimodal fit, respectively). The horizontal error bars represent the sum of the image width and the uncertainty in image location.

FNAL-HTR-OSU

Solving the wire quality and instability issue

- **What has been done:**
  - **Optimize wire design. The 2019 wires had very aggressive design, causing poor wire quality.**
  - **Use Nb alloy tubes with higher quality. Previous tubes had quality issue. New ATI tubes are better.**

2019 wire: aggressive recipe + old Nb alloy tube w/ low quality:

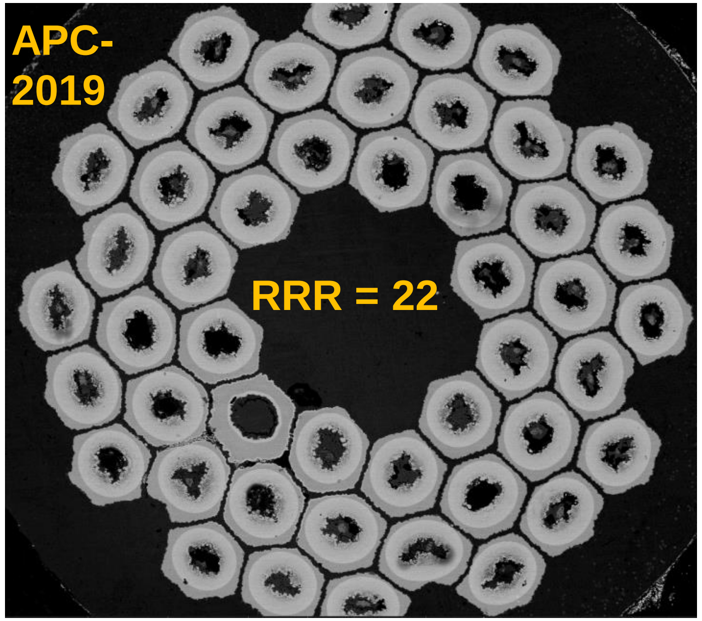

Recent wire, using ATI Nb-Ta-Hf:

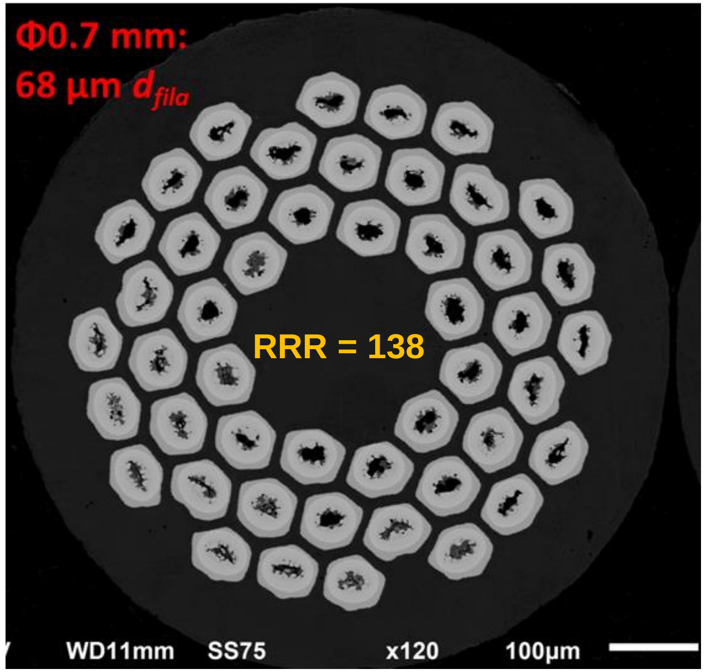

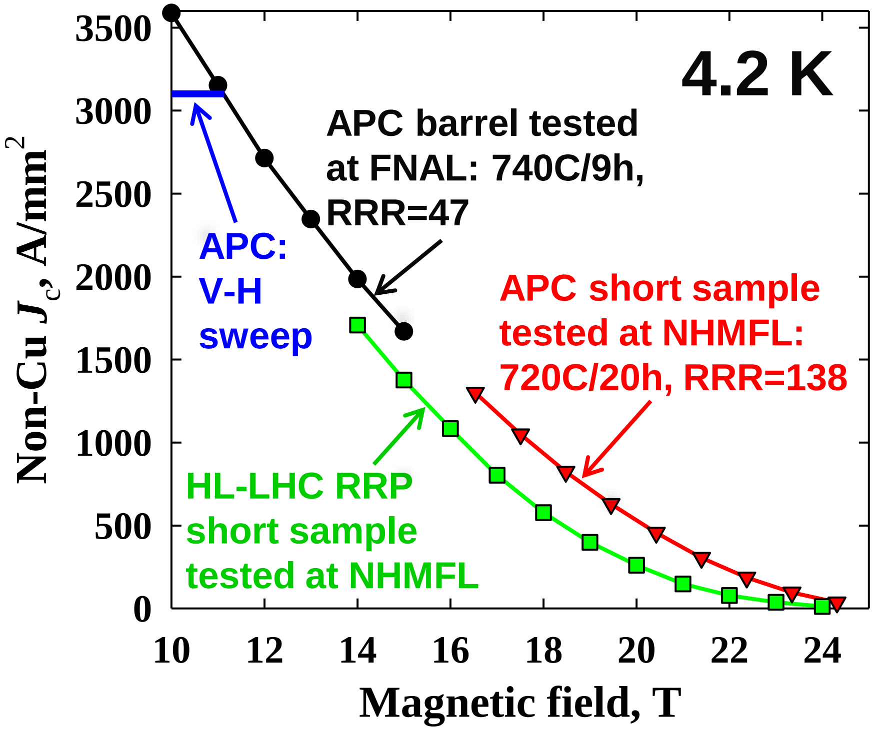

APC wires made using Nb-Ta-Hf seem to have lower $F_{p,max}$ and thus J_c than those using Nb-Ta-Zr.

- **Stability can be further improved by (1) optimizing heat treatment to increase RRR, (2) reducing filament size.**
- **Some instability was due to testing in the short sample form**

IEEE-CSC, ESAS and CSSJ SUPERCONDUCTIVITY NEWS FORUM (global edition), Issue No. 57, Oct 2024. Presentation given at ASC 2024, Sept 2024, Salt Lake City, Utah, USA.

New APC Nb_3Sn conductors with Optimized Recipe

FNAL-HTR-OSU

New-APC-1, 675 °C
(T4313, T4348, T4350)

Old-APC, 675 °C
(T4141, T4113)

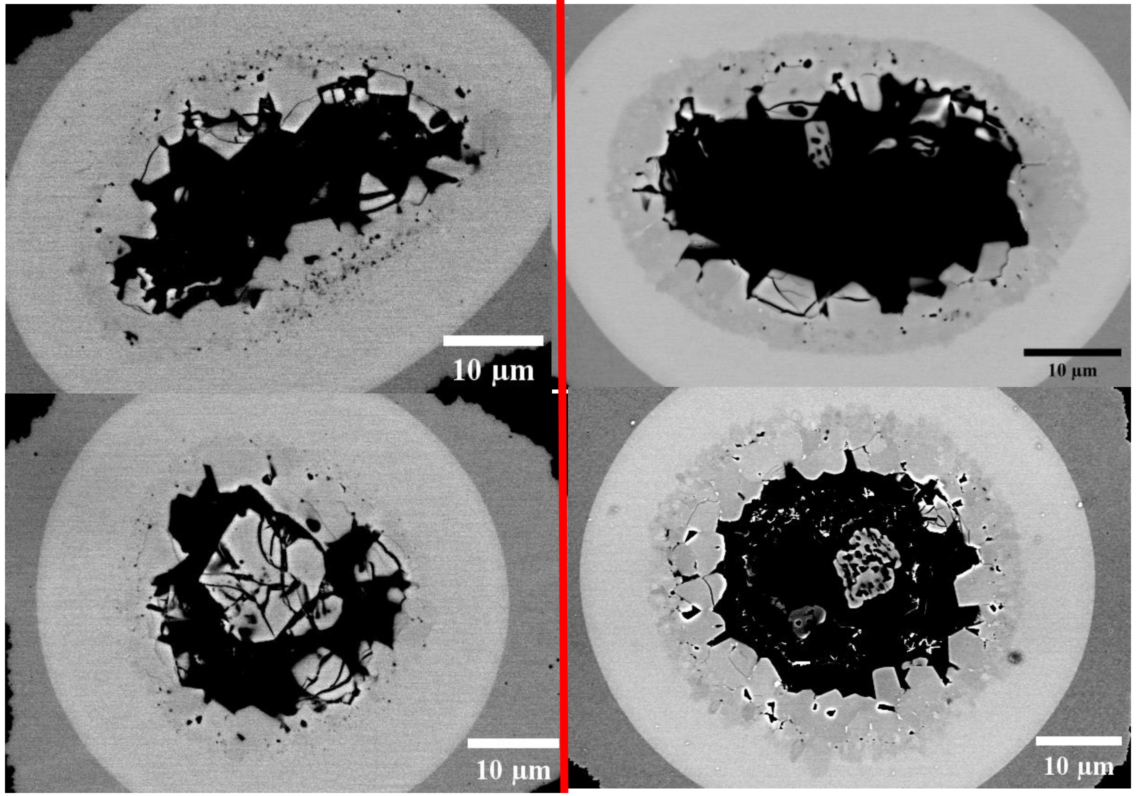

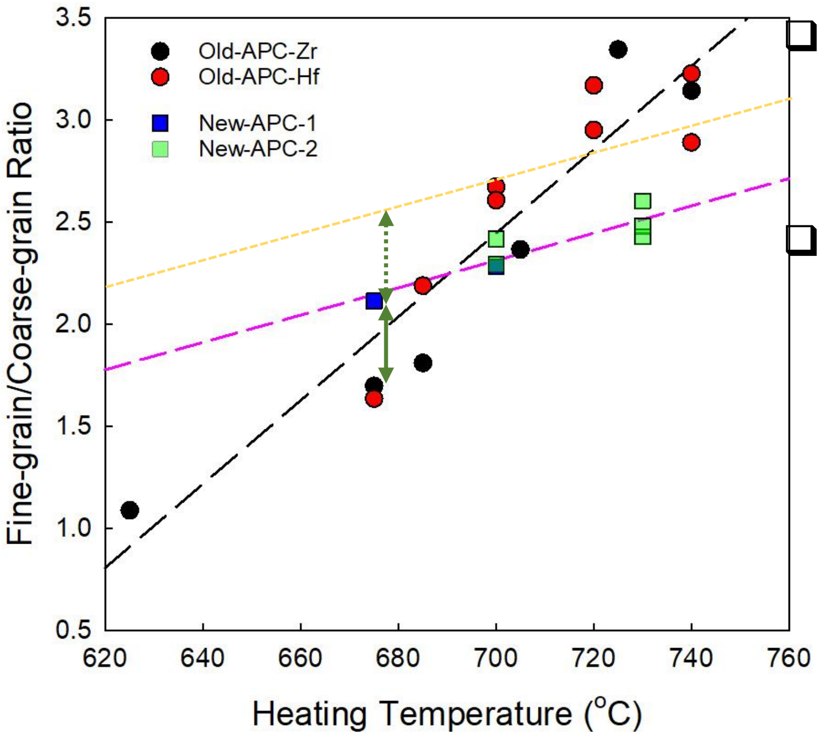

- New APCs have higher FG/CG ratio than old APCs at 675 °C
- Compared to old APCs, FG/CG ratio of new APCs decreases with decreasing heating temperature with a slower rate. In this case, new APCs have potential to attain higher FG/CG ratio than old APCs at low heating temperature

- In new APC reacted at 675 °C, disconnected CG regions were formed in some filaments. However, well-connected CG regions still exist in other filaments.

By further optimizing recipes of APC Nb_3Sn conductors:
It is expected that even higher FG/CG ratio can be achieved at low heating temperature.

IEEE-CSC, ESAS and CSSJ SUPERCONDUCTIVITY NEWS FORUM (global edition), Issue No. 57, Oct 2024. Presentation given at ASC 2024, Sept 2024, Salt Lake City, Utah, USA.

Enhanced Nb_3Sn with Hf induced Grain refinement

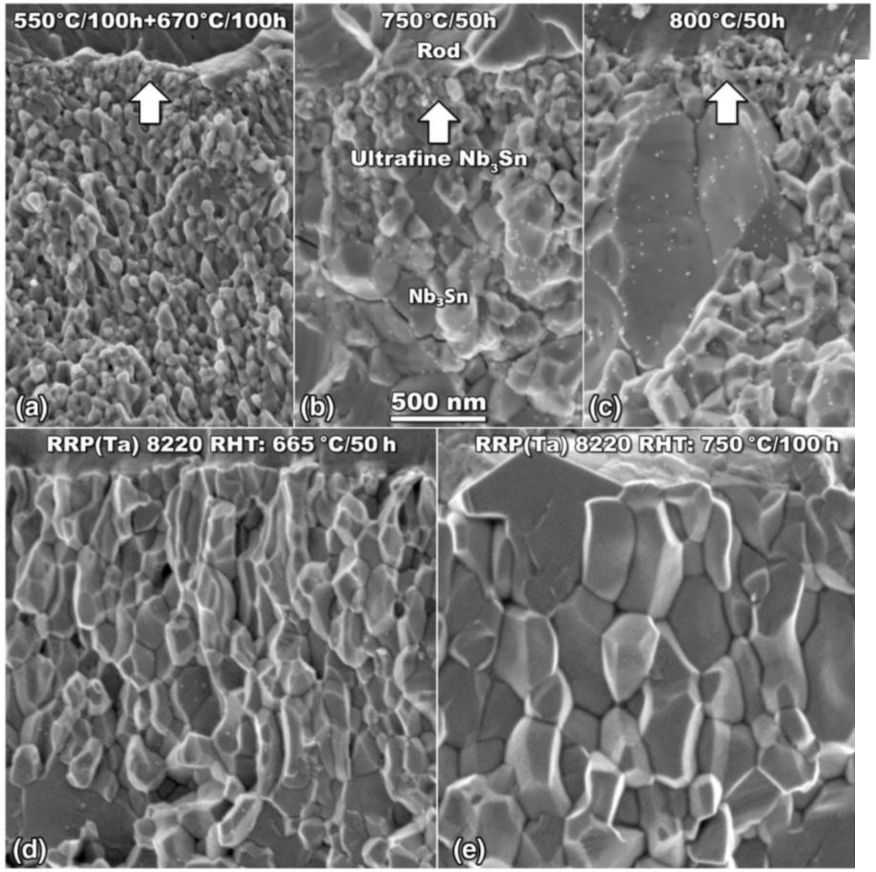

Figure 3. SEM characterization of Ta-Hf-doped Nb_3Sn compared with standard Ta-doped Nb_3Sn. Fractographs of Nb_3Sn grains after heat treatments at different temperature for Ta-Hf-doped samples made with home-made Nb4Ta1Hf special alloy (**a**–**c**) and for Ta-doped RRP wire made with industrial Nb4Ta (**d**,**e**).

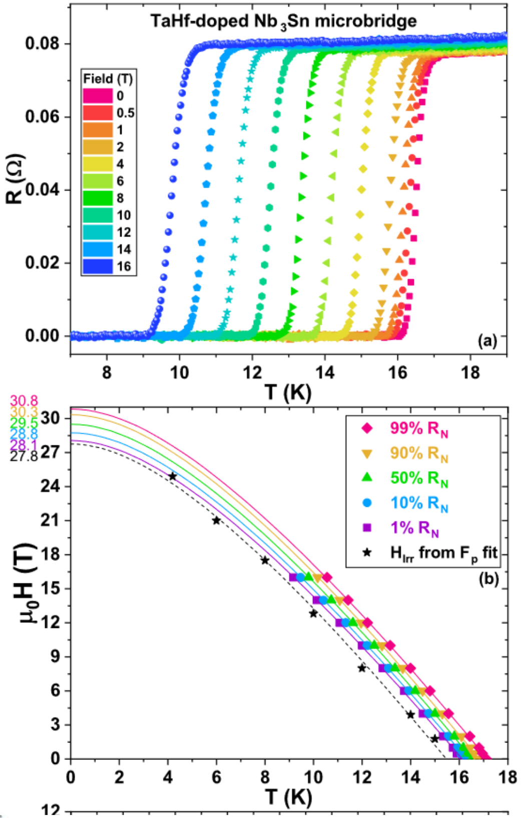

scientific reports

OPEN

Origin of the enhanced Nb_3Sn performance by combined Hf and Ta doping

Chiara Tarantini[1], Fumitake Kametani[1,2], Shreyas Balachandran[1], Steve M. Heald[3], Laura Wheatley[4], Chris R. M. Grovenor[4], Michael P. Moody[4], Yi-Feng Su[1,5], Peter J. Lee[1] & David C. Larbalestier[1,2]

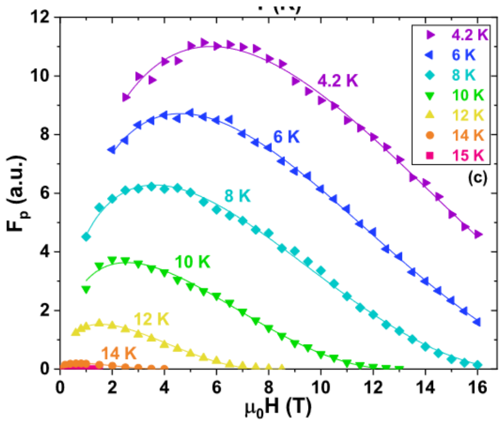

IEEE-CSC, ESAS and CSSJ SUPERCONDUCTIVITY NEWS FORUM (global edition), Issue No. 57, Oct 2024. Presentation given at ASC 2024, Sept 2024, Salt Lake City, Utah, USA.

FSU Group (Larbalestier, Tarantini)

Basic Understanding of B_{c2} in doped Nb_3Sn

PHYSICAL REVIEW MATERIALS **8**, 084801 (2024)

Influence of Nb alloying on Nb recrystallization and the upper critical field of Nb_3Sn

Nawaraj Paudel, Chiara Tarantini, Shreyas Balachandran,* William L. Starch, Peter J. Lee, and David C. Larbalestier†
Applied Superconductivity Center, National High Magnetic Laboratory, Florida State University, Tallahassee, Florida 32310, USA

(Received 16 May 2024; accepted 15 July 2024; published 1 August 2024)

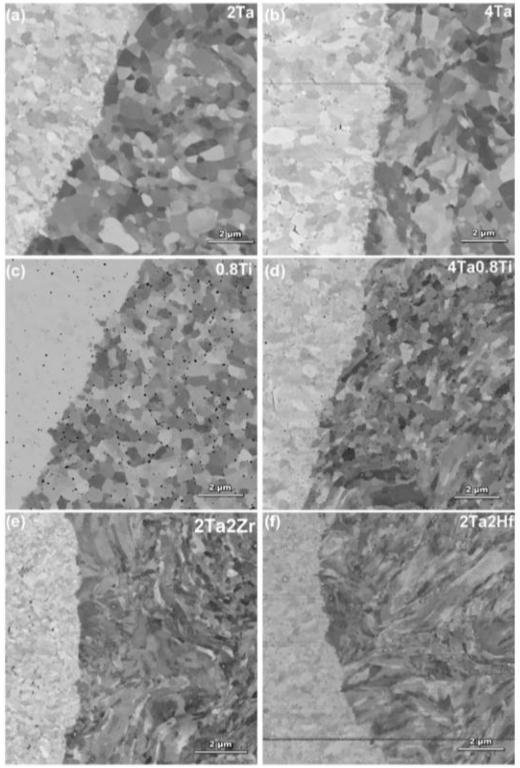

FIG. 5. Representative FESEM-BSE images of the Nb-alloy core/Nb_3Sn interface after the monofilaments were reacted at 550 °C/50 h+750 °C/50 h. The darker Nb-alloy cores are on the right and the lighter A15 diffusion layers are on the left of the interface (sample IDs are indicated in the top right corner of each image). Electron channeling contrast in the corresponding images reveals recrystallized microstructures in the unreacted NbxTa(x = 2, 4), Nb0.8Ti, and Nb4Ta0.8Ti alloys. In contrast, the Nb2Ta2Hf and Nb2Ta2Zr alloys retain a deformed, cold-worked grain structure.

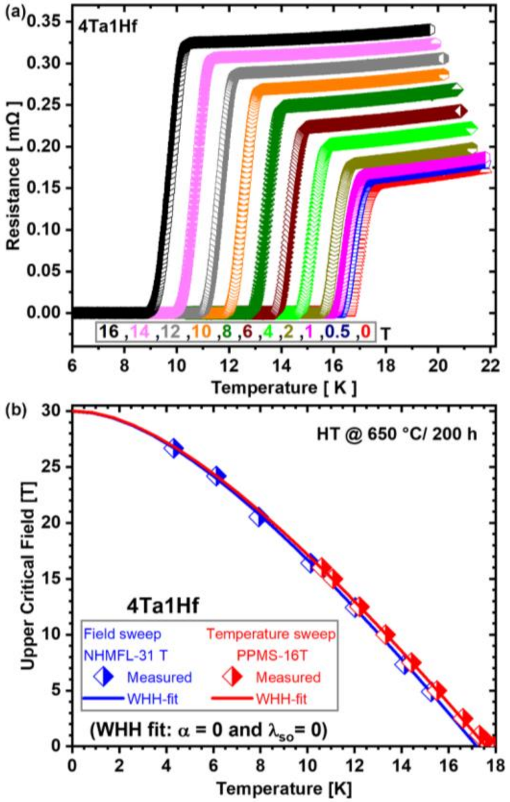

FIG. 6. (a) The traces of resistance against temperature using temperature sweeps at constant field from 0 to 16 T in our 16 T PPMS for Nb4Ta1Hf reacted at 550 °C/50 h+650 °C/200 h. (b) At the bottom we show the experimental $H_{c2}(T)$ values and their WHH fits in PPMS 16 T and NHMFL 31 T.

with the paramagnetic limitation parameter (α) and a spin-

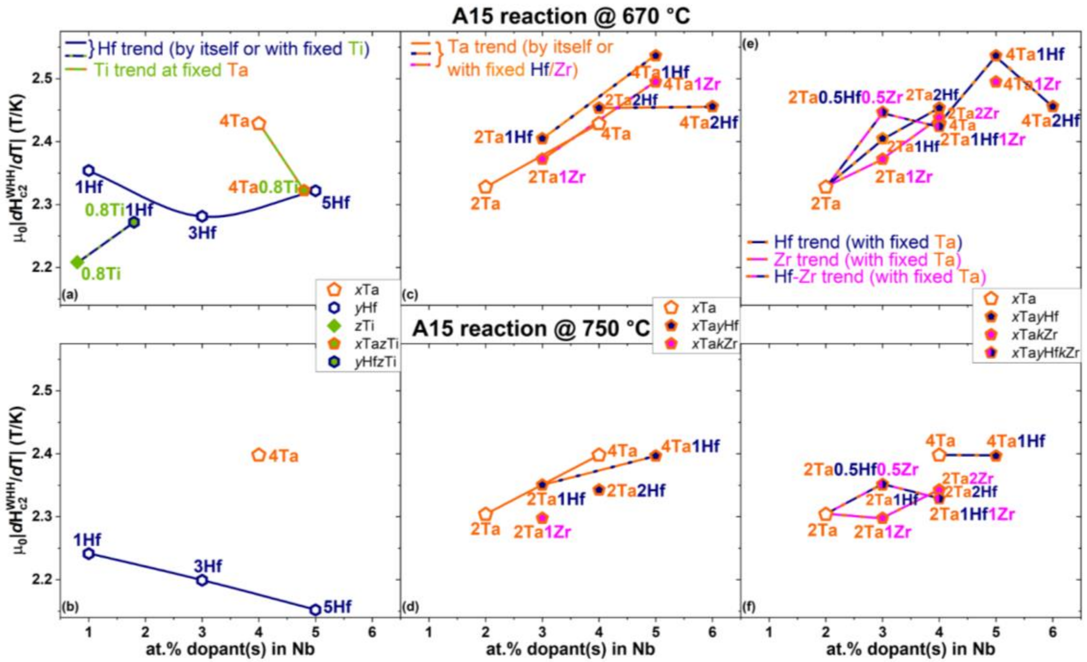

FIG. 8. H_{c2} slope evaluated by the WHH fits for alloyed A15 samples reacted at 550 °C/100 h+670 °C/100 h (top row) and at 550 °C/50 h+750 °C/50 h (bottom row) as a function of the amount of dopant(s). The same alloy sets as used for the (a)-(b), (c)-(d), and (d)-(e) columns in Fig. 7 are used for the column sets here. As explained in the text, the labels refer to the atomic percentage of dopant(s) in the unreacted Nb alloys.

Gianmarco BOVONE, Francesco LONARDO, Florin BUTA, Carmine SENATORE
UNIVERSITÉ DE GENÈVE FACULTÉ DES SCIENCES
Department of Quantum Matter Physics, University of Geneva, Switzerland
Department of Nuclear and Particle Physics, University of Geneva, Switzerland

Simon HOPKINS, Thierry BOUTBOUL
CERN, Switzerland

Internal Oxidation of test-bed Internal Sn subelements

Two possible configurations for the oxygen source

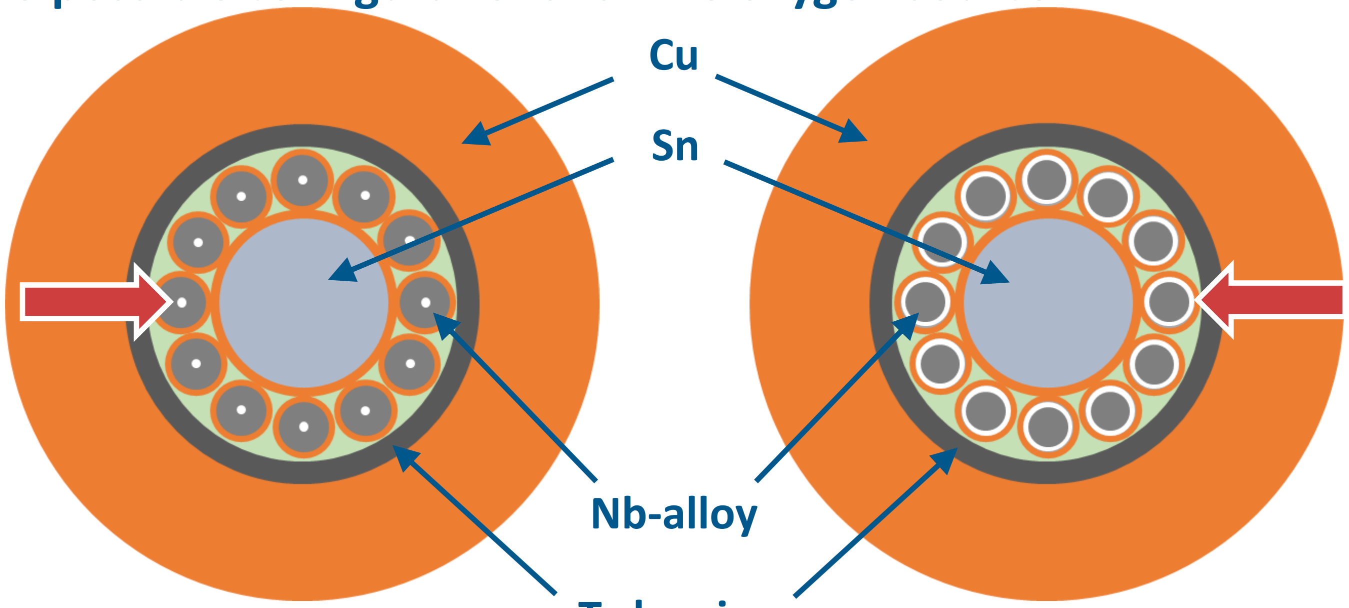

SnO_2 Core
SnO_2 powder inside the Nb-alloy filaments

SnO_2 Annular
SnO_2 powder between the Nb-alloy filaments and the Cu tube

Nb-alloy	Oxide configuration
Nb-7.5wt%Ta (REF.)	None
Nb-7.5wt%Ta-1wt%Zr	None
	SnO_2 Core
Nb-7.5wt%Ta-2wt%Hf	None
	SnO_2 Core
	SnO_2 Annular

Two commercial ternary alloy were tested with 1wt%Zr and 2wt%Hf

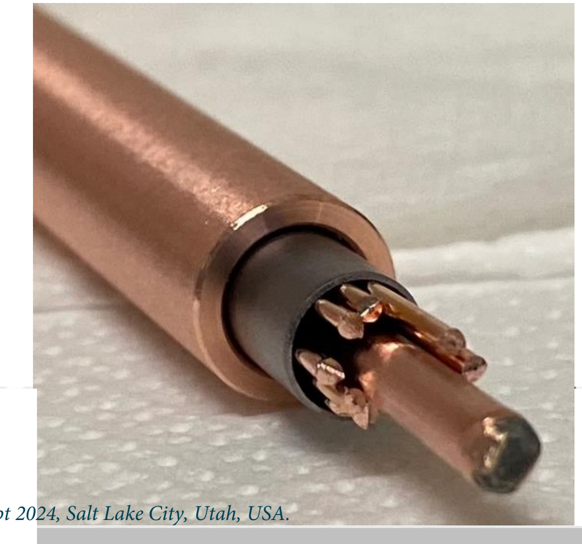

G. Bovone *et al.,* Supercond. Sci. Tech. 36 (2023) 095018
DOI: 10.1088/1361-6668/aced25

IEEE-CSC, ESAS and CSSJ SUPERCONDUCTIVITY NEWS FORUM (global edition), Issue No. 57, Oct 2024. Presentation given at ASC 2024, Sept 2024, Salt Lake City, Utah, USA.

HT: 550°C x 100h + 650°C x 200h

Internal Oxidation of test-bed Internal Sn subelements

12-filament wires with an internal Sn source

w/o oxygen source | SnO_2 Core | SnO_2 Annular

Nb-7.5wt%Ta-1wt%Zr

Nb-7.5wt%Ta-2wt%Hf

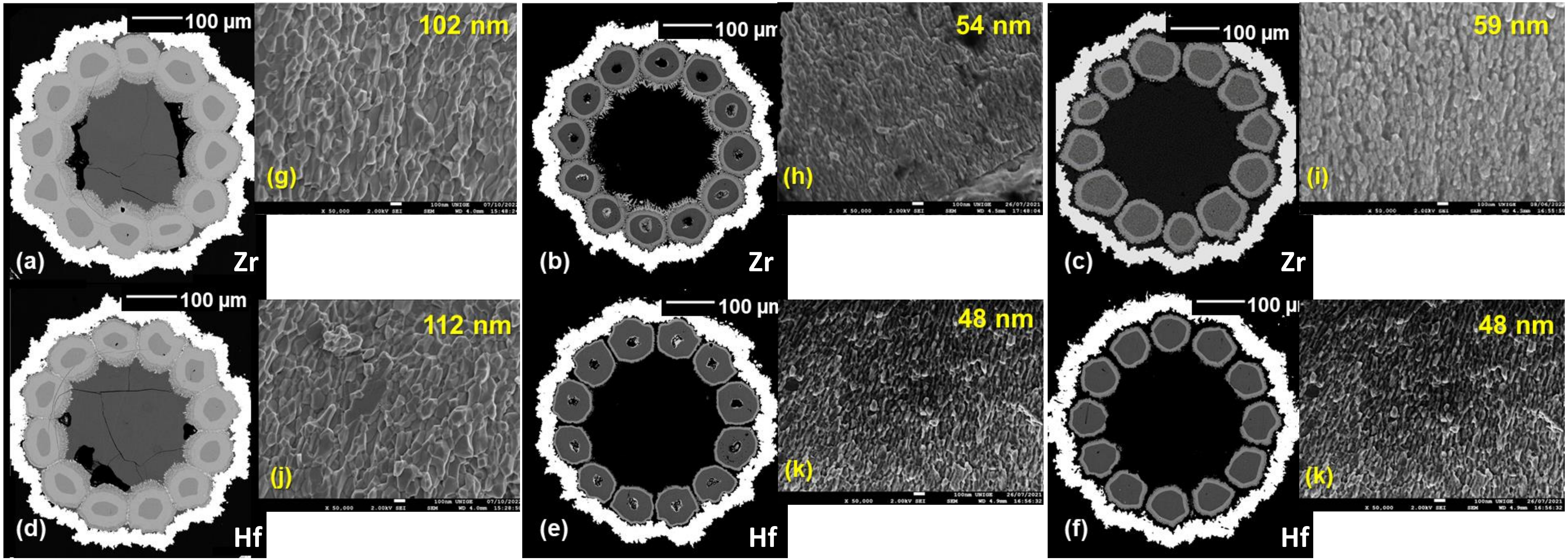

Internal oxidation leads to a refinement of the grain size from ~100 nm to ~50 nm regardless of the oxygen source configuration

G. Bovone *et al.*, Supercond. Sci. Tech. 36 (2023) 095018
DOI: 10.1088/1361-6668/aced25

Internal Oxidation of test-bed Internal Sn subelements

Transport I_c and B_{c2} measurements

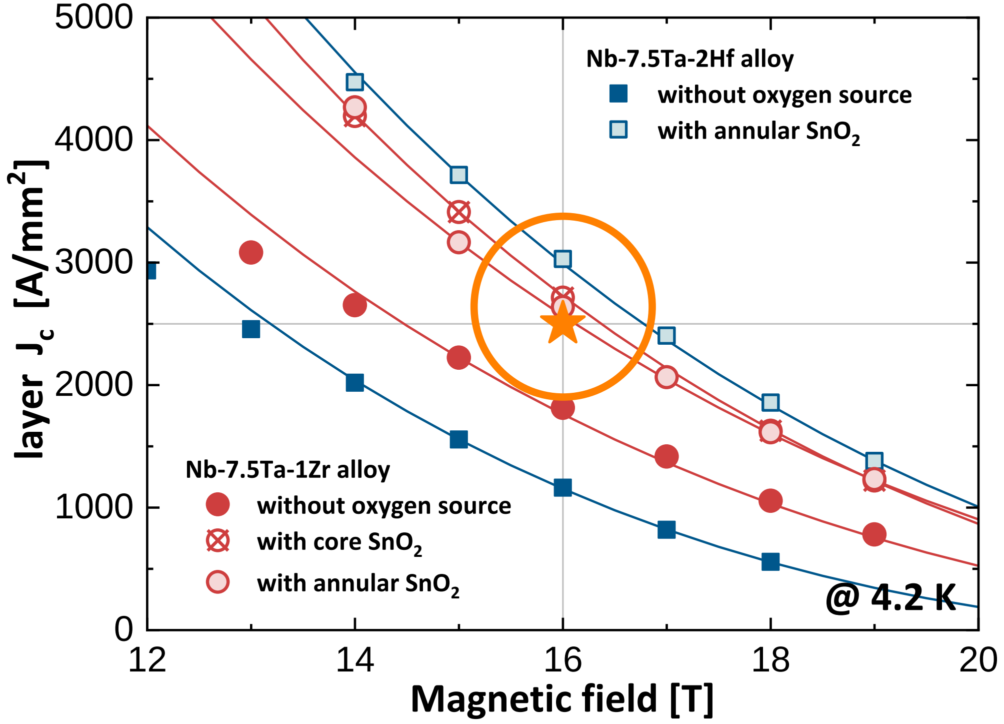

Layer J_c determined from transport measurements

FCC layer J_c (4.2K,16T) = 2’500 A/mm^2 considering 60% of Nb_3Sn in the non-Cu area

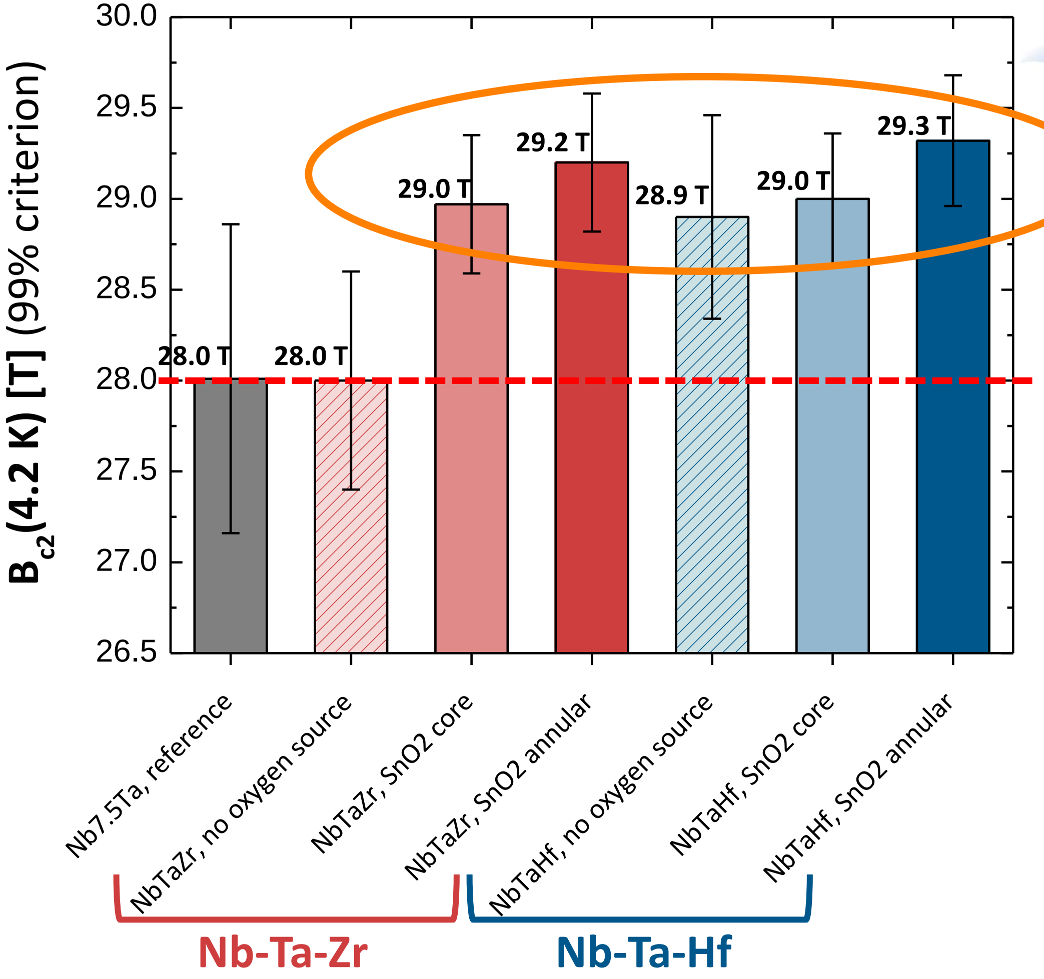

R(B) tests performed up to 33 T at LNCMI-Grenoble confirm that the record high B_{c2} values are achieved both with Hf and Zr

G. Bovone *et al.*, Supercond. Sci. Tech. 36 (2023) 095018
DOI: 10.1088/1361-6668/aced25

IEEE-CSC, ESAS and CSSJ SUPERCONDUCTIVITY NEWS FORUM (global edition), Issue No. 57, Oct 2024. Presentation given at ASC 2024, Sept 2024, Salt Lake City, Utah, USA.

Exceptional High H_{c2} and H_{Irr} in alloyed Nb_3Sn bulk samples

Manish Mandal, Chiara Tarantini, William L Starch, Peter J Lee, and David C Larbalestier
Florida State University

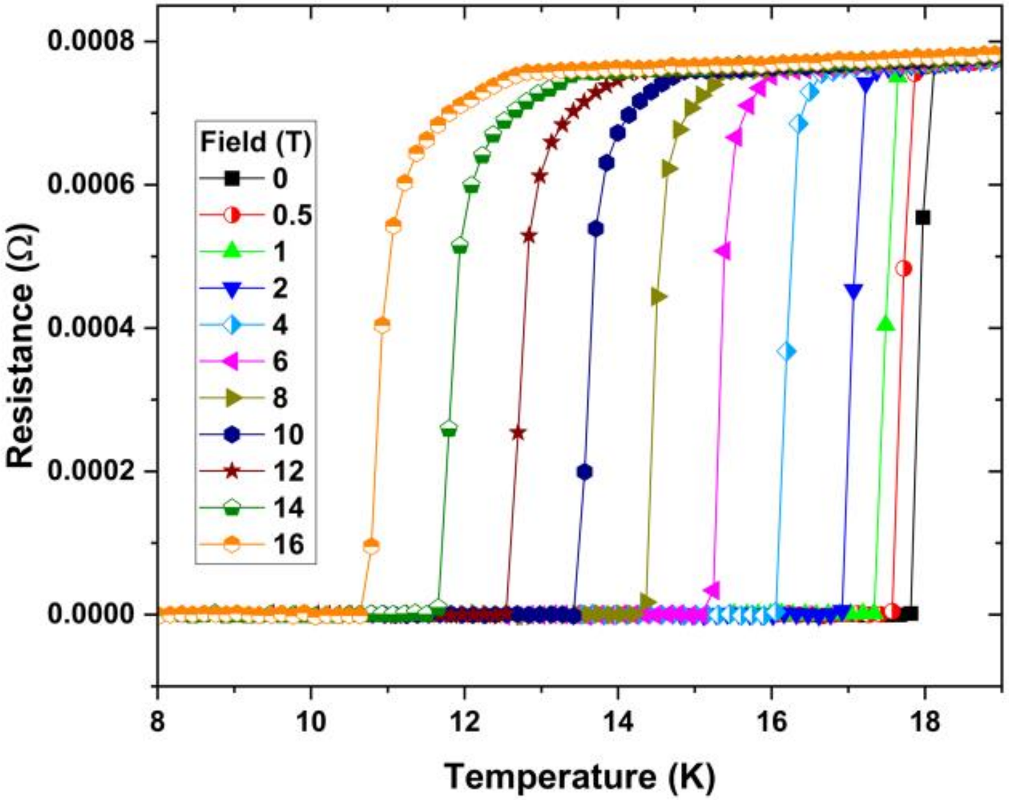

$\mu_0 H_{c2,99\%}(0) = 39.2$ T

$\mu_0 H_{Irr,1\%}(0) = 30.0$ T

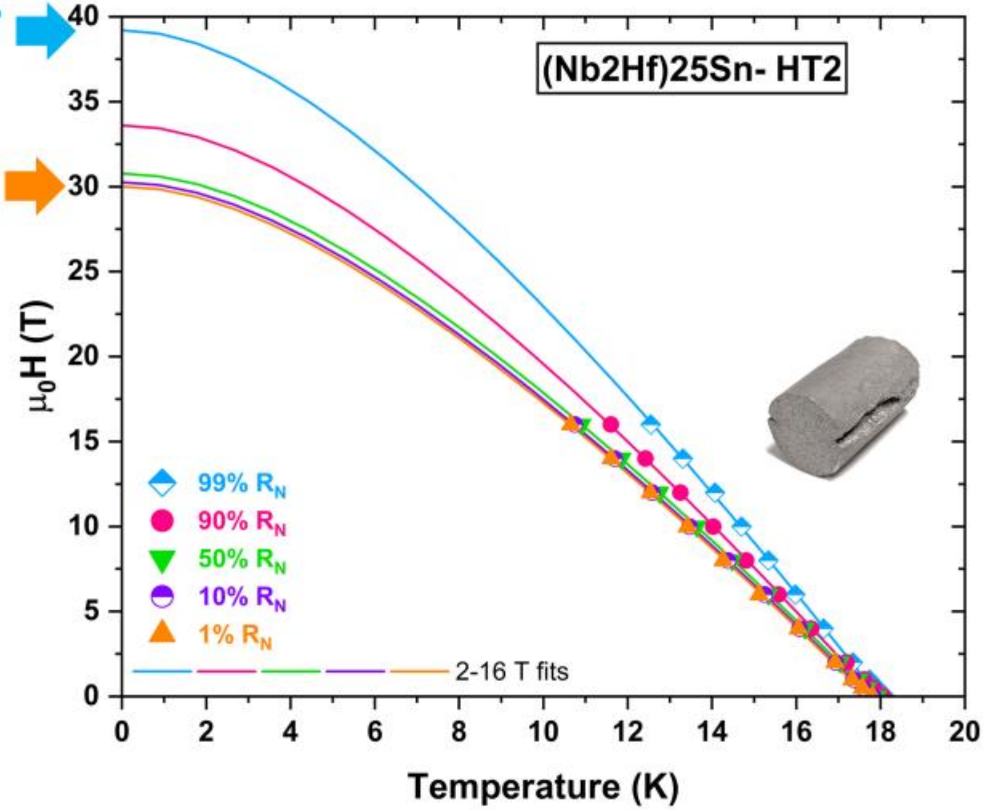

WHH extrapolations to 0 K

M. Mandal's poster: 4MPo1B-06

Conclusions and Take home Message

- LTSC have great continuing utility in commercial and technical/scientific applications
- They will be used for a number of future accelerator and fusion programs
- The have some potentially interesting new niche applications
- They have continuing potential for property improvement – as evidenced by a number of recent and exciting new results
- They can be expected to complement HTSC conductors moving forward